August 2022

Name & Qualifications
Associate Professor Marnie Forster

Department / School / Centre
College of Science
Research School of Earth Sciences
Argon Facility
+61 425603412
Marnie.forster@anu.edu.au

Canberra ACT 0200 Australia
www.anu.edu.au

CRICOS Provider No. 00120C

ANU Argon Facility Technical Report: ANU13-2020

$^{40}Ar/^{39}Ar$ Analysis
For NATIONAL ARGON MAP
By Marnie Forster and Davood Vasegh

NAM PROJECTS 02 & 03:
TITLES:

P02: **Dating of mineralisation-related alteration in the Olympic Cu-Au Province, Gawler Craton**

P03: **Dating of mineralisation-related alteration at the Cairn Hill Mine, and regional thermal history of the northern Mt Woods Region, Gawler Craton**

This project was enabled by NCRIS via AuScope

This work has been undertaken to support MinEx CRC

Sample Provider	Anthony Reid (Geological Survey of South Australia)
Financial Contributor	Argon Analysis: AuScope Mineral Separation: GSSA
Mineral Separation	Mineral Separation Facility at Research School of Earth Sciences, ANU
Analysis Methodology & Interpretation	Marnie Forster at ANU Argon Facility
Sample Analysis	Davood Vasegh at ANU Argon Facility
Data Reduction	Davood Vasegh at ANU Argon Facility
Supplementary Information	Marnie Forster and Davood Vasegh at ANU Argon Facility

Proposal 2:

Dating of mineralisation-related alteration in the Olympic Cu-Au Province, Gawler Craton

Geographic Region: Olympic Cu-Au Province
Geological Province: Gawler Craton

The Olympic Cu-Au Province is a metallogenic province in South Australia that contains one of the world's most significant Cu-Au-U resources in the Olympic Dam deposit. The Olympic Cu-Au Province also hosts a range of other iron oxide-copper-gold (ICOG) deposits including the Prominent Hill and Carrapateena deposits. Previous thermochronology work within the region of the Olympic Dam deposit has demonstrated that the mineralising event at c. 1590 Ma is also recorded as a thermal event by biotite and muscovite in country rocks of the region (Skirrow et al., 2007). However, to the north east of Olympic Dam, $^{40}Ar/^{39}Ar$ dating of hydrothermal K-feldspar suggests that younger events have also modified the crust in this region, with evidence for c. 1.3 – 1.1 Ga fluid flow (Reid et al., 2017). The thermal evolution of the Olympic Cu-Au Province is poorly constrained and the influence of younger events poorly known.

This proposal seeks to build on the 3 existing $^{40}Ar/^{39}Ar$ analyses from the region around Olympic Dam with two more samples. The first is from a hematite altered but unmineralised granite in the vicinity of Olympic Dam. The second is an altered granite in the vicinity of the Oak Dam prospect.

Sample information from proposal and locations:

Two samples only.

Sample number	Location	MGA East	MGA North	Zone	Target mineral	Lithology
2131356	DH ASD 1	701270	6564445	53	muscovite	altered granite
2111462	Blanche 1	672516	6627750	53	K-feldspar, muscovite	altered granite

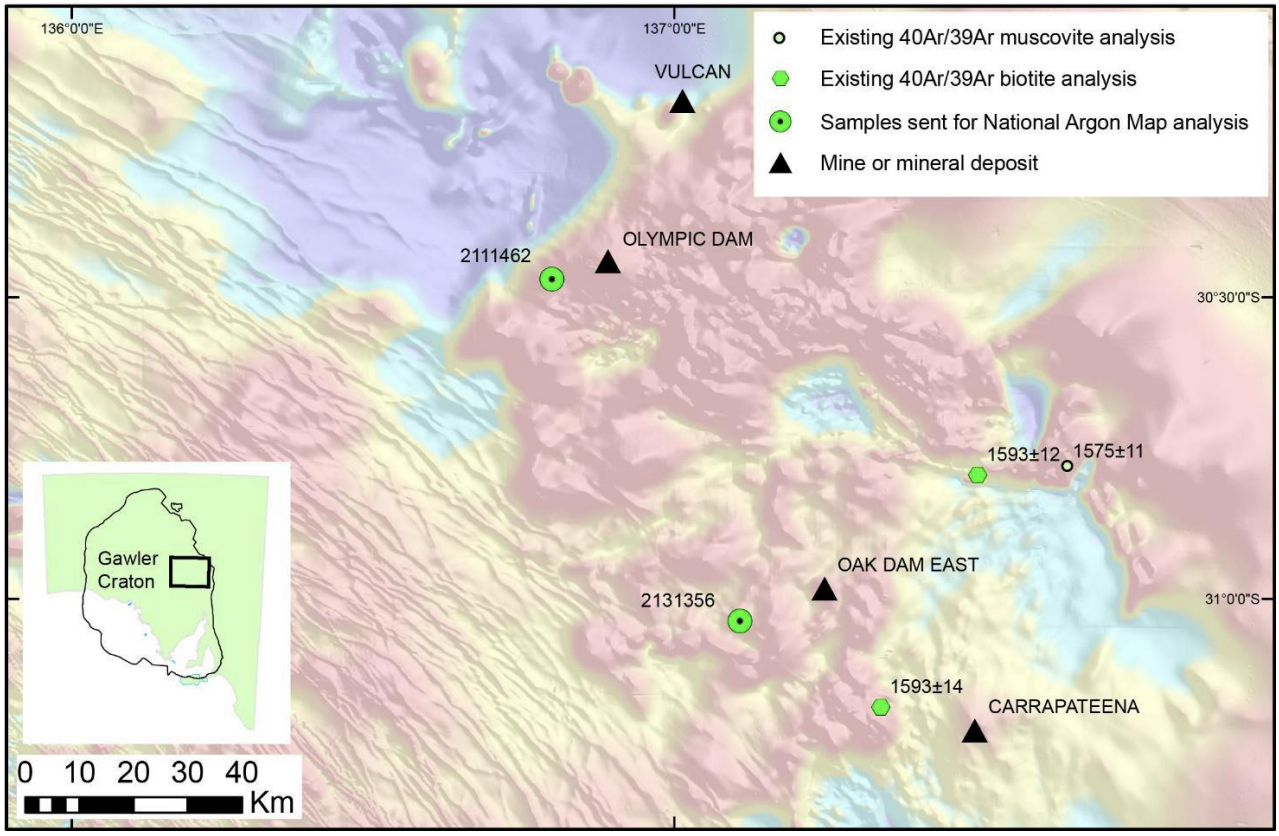

Location map of samples submitted for this National Argon Map application. Note the samples of biotite in the vicinity of Carrapateena and Oak Dam East are from Skirrow et al. (2007).

Sample Description

Sample 2131356 is an altered granite from drill hole ASD 1. The granite is hematite altered and the muscovite is medium to fine grained. The analysis of K-feldspar in this sample and or muscovite may provide constraints as to the timing of the alteration in the region to the east of Oak Dam Oak Dam is a major new discovery by BHP in the region. Previous analysis of K-feldspar by the laser ablation methods yielded ages c. 900 – 600 Ma, while coexisting muscovite yielded an age of c. 1533 Ma.

Sample 2111462 is a coarse-grained granite from geothermal drill hole Blache 1. Previous dating from this drill hole was attempted by Hall et al. (2018), who analysed apatite via U-Pb and fission track methods. The

$^{40}Ar/^{39}Ar$ analysis plots and information

The age plots are interpreted using the Asymptote and Limits method (Forster and Lister 2004). The argon system is affected by heat, for example if a sample is heated long enough then the argon system will be completely reset, if however, it is heated for a relatively short period of time and/or with temperatures that are not extreme then the sample may be only partially reset. Thus, relic ages can be retained and likewise overprinting events can be recorded and not overprint the argon system completely. As a consequence, the argon plots can have more than one 'age'. In many cases a minor overprinting event can be seen in these plots, it will be a maximum age and not necessary an accurate age but does show that a younger overprinting event did occur. It can be seen in the age plots that after the steps that record the youngest event, they are followed by diffusional loss and/or mixing towards the older ages that are highlighted in blue or green.

The argon data results are presented as Apparent Age Plots. The age data is presented on these plots showing the ages for different populations within each sample. Each age is highlighted and has a dashed orange line. defined shows the error, the MSWD, the steps representing the % gas release, and the Pearsons chi statistics for each of these domains is presented where applicable. There are commonly 3 ages defined on each spectrum: 1) the minor age defined (brown) at the low temperature of the experiment shows that there has been a minor overprinting event, but this age is not accurate and is only defined by e.g. <2% gas release. 2) an intermediate domain (green), commonly this is the major gas release; 3) a relict domain age (blue) that has been preserved showing an older history occurred. The intervening steps that are tan or clear represent mixing steps and are a normal phenomenon. In addition, there is the sample identification number; the foil number; the mineral; the ANU canister number; the mass used and the number of steps. At the base of the plot is the sample information e.g. location.

Summary: Each of the selected interpreted ages have been labelled with a dashed orange line and the age and age data placed on that line. This includes the age, the calculated error, the MSWD and all to 95% c.l. These blue or green selected steps represent an age population. Note that in several cases the mixing steps are yellow (this is a software aspect and is meaningless).

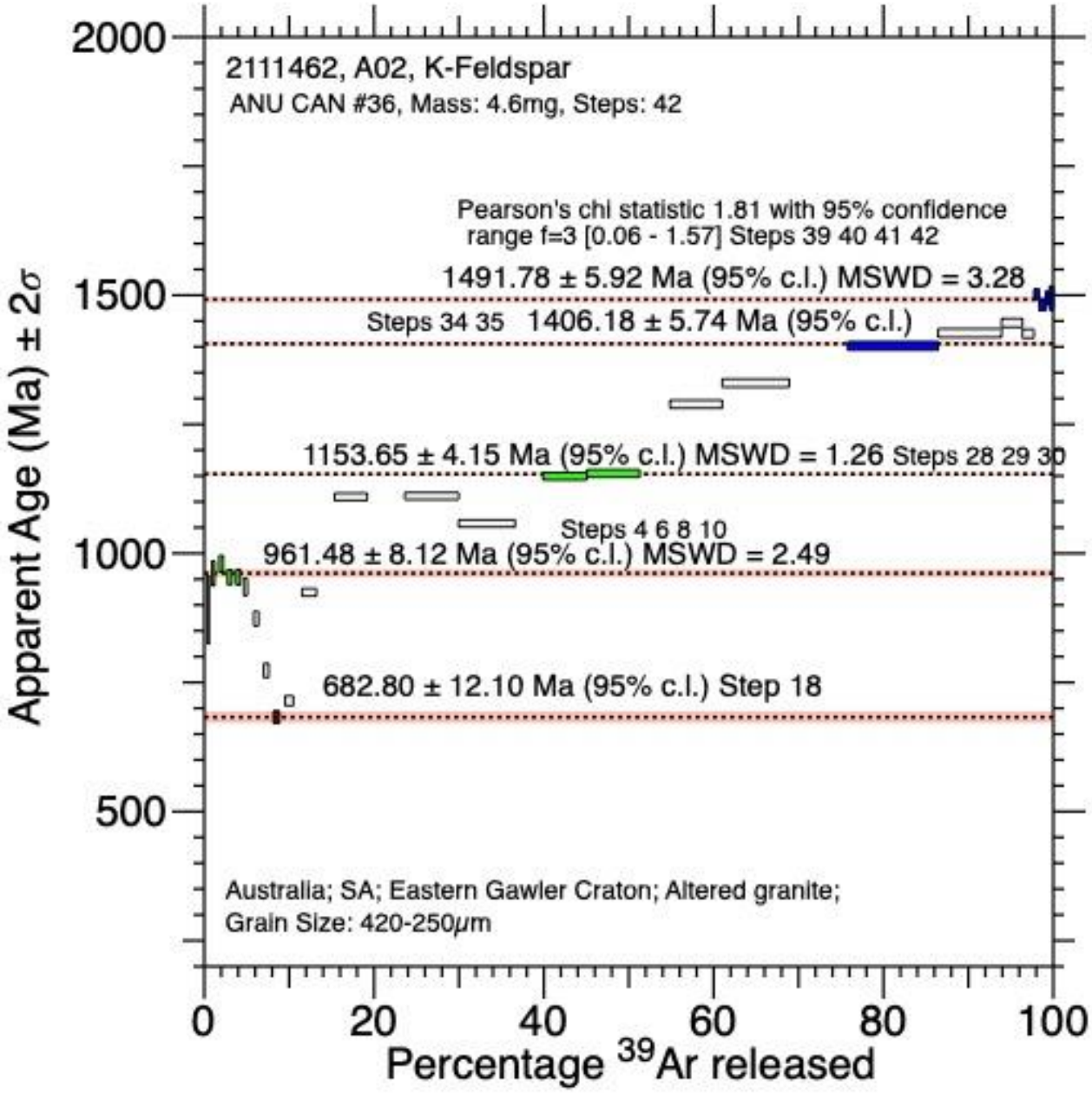
2111462, A02, K-Feldspar
ANU CAN #36, Mass: 4.6mg, Steps: 42
Pearson's chi statistic 1.81 with 95% confidence
range f=3 [0.06 - 1.57] Steps 39 40 41 42
1491.78 ± 5.92 Ma (95% c.l.) MSWD = 3.28
Steps 34 35 1406.18 ± 5.74 Ma (95% c.l.)
1153.65 ± 4.15 Ma (95% c.l.) MSWD = 1.26 Steps 28 29 30
Steps 4 6 8 10
961.48 ± 8.12 Ma (95% c.l.) MSWD = 2.49
682.80 ± 12.10 Ma (95% c.l.) Step 18
Australia; SA; Eastern Gawler Craton; Altered granite;
Grain Size: 420-250μm
Apparent Age (Ma) ± 2σ
2000
1500
1000
500
0
20
40
60
80
100
Percentage 39Ar released

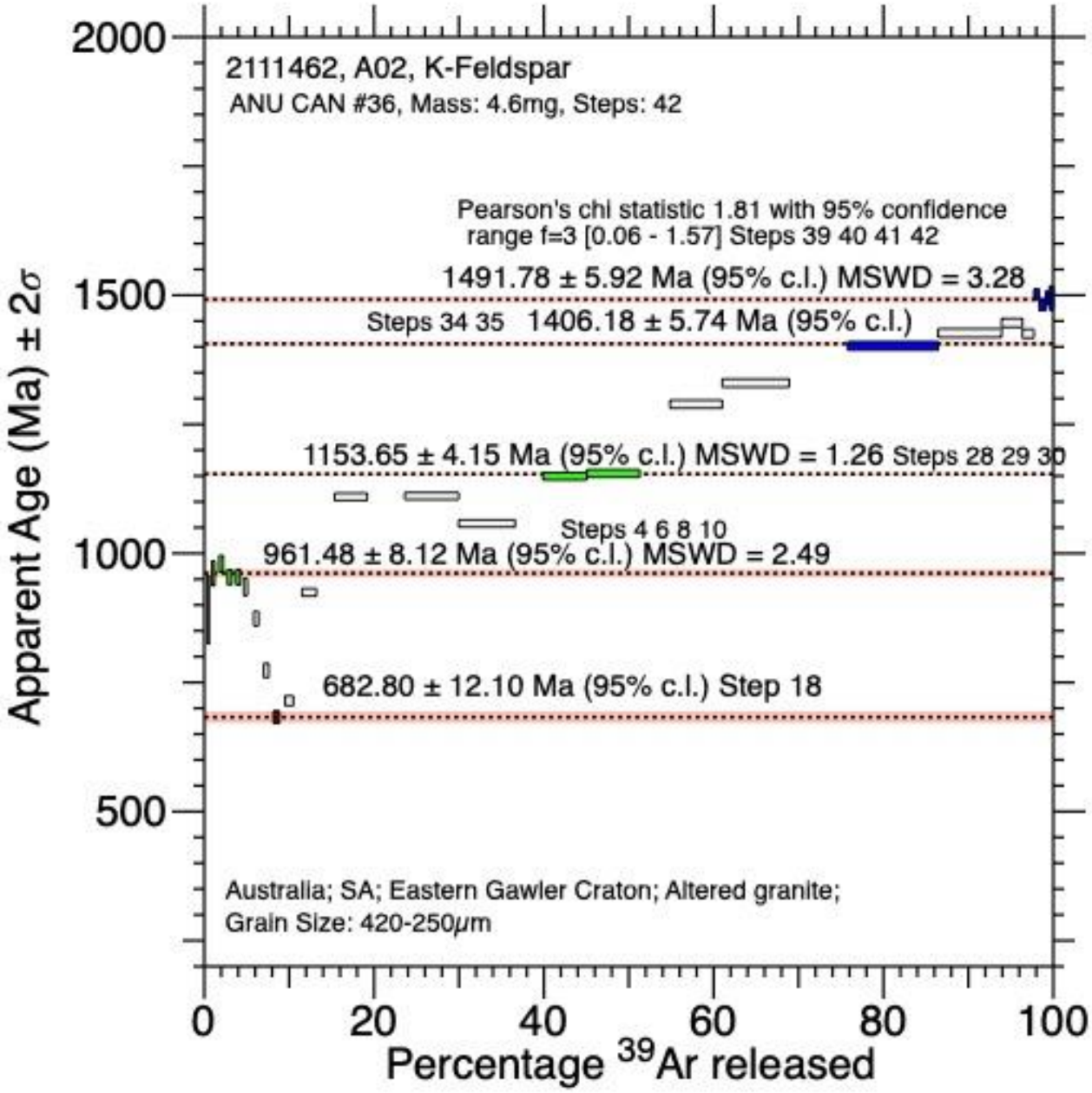
2111462, A02, K-Feldspar
ANU CAN #36, Mass: 4.6mg, Steps: 42
Pearson's chi statistic 1.81 with 95% confidence
range f=3 [0.06 - 1.57] Steps 39 40 41 42
1491.78 ± 5.92 Ma (95% c.l.) MSWD = 3.28
Steps 34 35 1406.18 ± 5.74 Ma (95% c.l.)
1153.65 ± 4.15 Ma (95% c.l.) MSWD = 1.26 Steps 28 29 30
Steps 4 6 8 10
961.48 ± 8.12 Ma (95% c.l.) MSWD = 2.49
682.80 ± 12.10 Ma (95% c.l.) Step 18
Australia; SA; Eastern Gawler Craton; Altered granite;
Grain Size: 420-250μm
Apparent Age (Ma) ± 2σ
2000
1500
1000
500
0
20
40
60
80
100
Percentage 39Ar released

Additional plots:

The following pages include nine different plots for each sample:

- Apparent Age Spectrum
- Arrhenius Plot (these are an estimate only).
- r/r0 Plot
- Percentage Radiogenic Argon
- Ca/K Plot
- Cl/K Plot
- Turner Plot

These are provided to enhance the understanding of the analytical results.

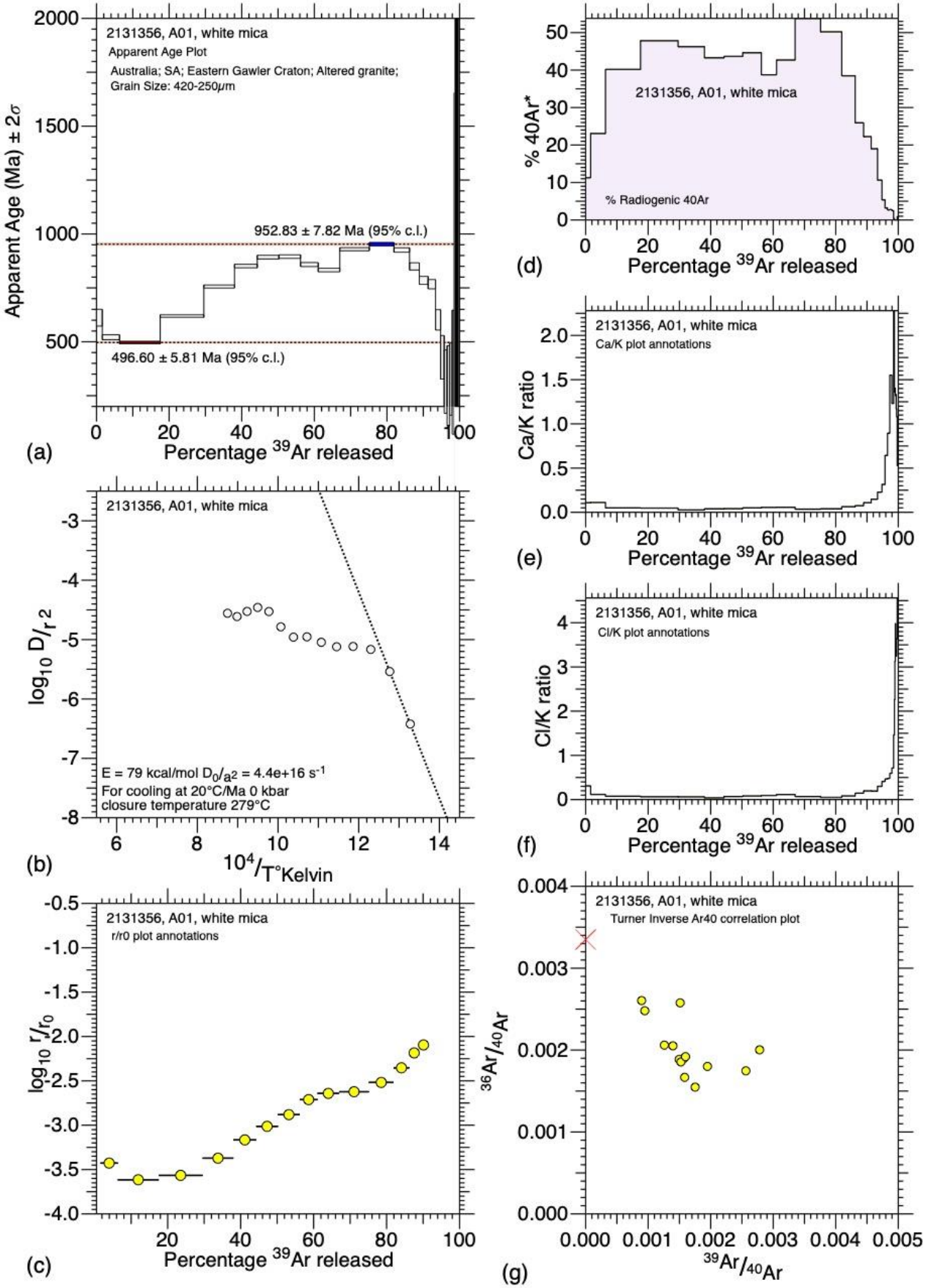
2131356, A01, white mica
Apparent Age Plot
Australia; SA; Eastern Gawler Craton; Altered granite;
Grain Size: 420-250μm
952.83 ± 7.82 Ma (95% c.l.)
496.60 ± 5.81 Ma (95% c.l.)
Apparent Age (Ma) ± 2σ
Percentage 39Ar released
(a)
2131356, A01, white mica
E = 79 kcal/mol D0/a2 = 4.4e+16 s-1
For cooling at 20°C/Ma 0 kbar
closure temperature 279°C
log10 D/r2
10^4/T°Kelvin
(b)
2131356, A01, white mica
r/r0 plot annotations
log10 r/r0
Percentage 39Ar released
(c)
2131356, A01, white mica
% Radiogenic 40Ar
% 40Ar*
Percentage 39Ar released
(d)
2131356, A01, white mica
Ca/K plot annotations
Ca/K ratio
Percentage 39Ar released
(e)
2131356, A01, white mica
Cl/K plot annotations
Cl/K ratio
Percentage 39Ar released
(f)
2131356, A01, white mica
Turner Inverse Ar40 correlation plot
36Ar/40Ar
39Ar/40Ar
(g)

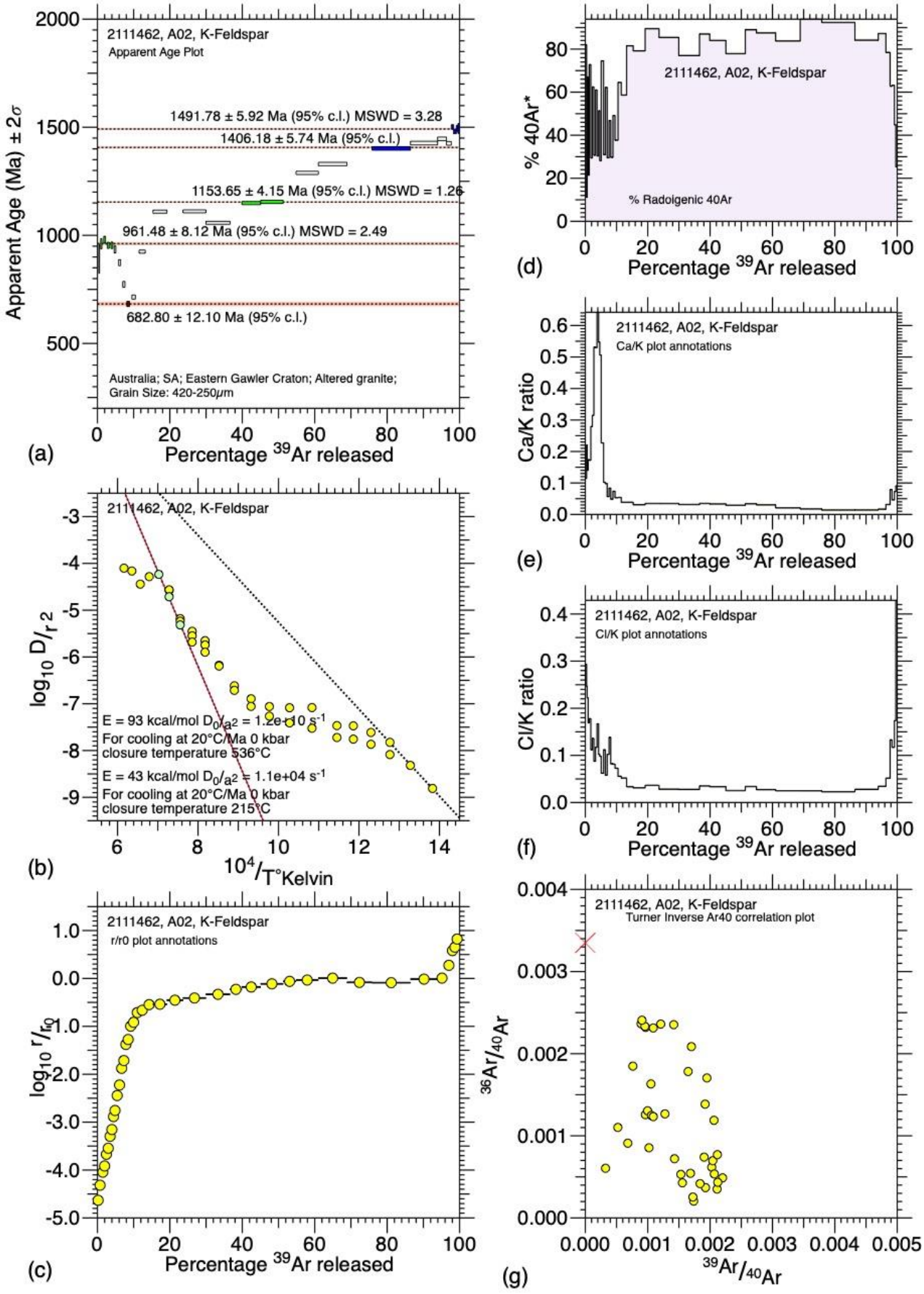
2111462, A02, K-Feldspar
Apparent Age Plot
1491.78 ± 5.92 Ma (95% c.l.) MSWD = 3.28
1406.18 ± 5.74 Ma (95% c.l.)
1153.65 ± 4.15 Ma (95% c.l.) MSWD = 1.26
961.48 ± 8.12 Ma (95% c.l.) MSWD = 2.49
682.80 ± 12.10 Ma (95% c.l.)
Australia; SA; Eastern Gawler Craton; Altered granite;
Grain Size: 420-250μm
Apparent Age (Ma) ± 2σ
Percentage 39Ar released
(a)
2111462, A02, K-Feldspar
E = 93 kcal/mol D0/a2 = 1.2e+10 s-1
For cooling at 20°C/Ma 0 kbar
closure temperature 536°C
E = 43 kcal/mol D0/a2 = 1.1e+04 s-1
For cooling at 20°C/Ma 0 kbar
closure temperature 215°C
log10 D/r2
10^4/T°Kelvin
(b)
2111462, A02, K-Feldspar
r/r0 plot annotations
log10 r/r0
Percentage 39Ar released
(c)
2111462, A02, K-Feldspar
% Radolgenic 40Ar
% 40Ar*
Percentage 39Ar released
(d)
2111462, A02, K-Feldspar
Ca/K plot annotations
Ca/K ratio
Percentage 39Ar released
(e)
2111462, A02, K-Feldspar
Cl/K plot annotations
Cl/K ratio
Percentage 39Ar released
(f)
2111462, A02, K-Feldspar
Turner Inverse Ar40 correlation plot
36Ar/40Ar
39Ar/40Ar
(g)

Proposal 3:

Dating of mineralisation-related alteration at the Cairn Hill Mine, and regional thermal history of the northern Mt Woods Region, Gawler Craton

Geographic Region: Mt Woods Regions
Geological Province: Gawler Craton

The Cairn Hill Fe-Cu deposit is an example of magnetite-dominant iron oxide copper gold (IOCG) mineralisation in the Gawler Craton. Hematite-dominant IOCG deposits are well represented within the Olympic Cu-Au Province, including Olympic Dam, Prominent Hill and Carapateena (Skirrow et al. 2007; Skirrow 2009). Magnetite IOCG's are less common, with Cairn Hill the only deposit of economic viability in South Australia.

Previous work at Cairn Hill has dated two rock types by zircon U-Pb (Jagodzinski and Reid, 2015). The host monzogranite has a tectonic fabric defined by elongate quartz ribbons and the alignment of the minor biotite. This rock was emplaced at 1572 ± 6 Ma. A second sample of unmineralised and weakly deformed microgranite was emplaced at 1514 ± 8 Ma.

The mineralisation is magnetite-rich and associated with apatite-amphibole-phlogopite alteration. A previous attempt to date the amphibole (hornblende) and phlogopite was made via laser ablation $^{40}Ar/^{39}Ar$ methods (Jagodzinski and Reid, 2015). However, due to rapid outgassing of both the hornblende and phlogopite, both age spectra is dominated by single steps, which yielded ages c. 1490 Ma and c. 1460 Ma respectively. This proposal is to date the hornblende and phlogopite in the alteration via furnace step heating methods to refine this age and our understanding of magnetite-rich IOCG mineral systems in the northern Gawler Craton.

In addition we also submit a second sample of biotite gneiss from drill hole KDD005.This is an example of the regional host rock in the vicinity of the Cairn Hill mine and will enable the characterisation of the cooling history of the region that can be compared with the analysis or hornblende from the mineralisation itself.

These new samples compliment two samples of biotite analysed by Fraser et al. (2012) which are in the vicinity of the Cairn Hill mine, and yielded ages of 1490 ± 8 Ma (sample 2007371062, Biotite gneiss CD93 2 175.7–176.0m) and 1444 ± 5 Ma (sample 2007371063, Granitic gneiss, DD86EN33
85.1–85.3m). In addition, there are also four samples of biotite analysed by Forbes et al. (2012) from elsewhere in the Mt Woods region. These ages are older than the biotite dated by Fraser et al. (2012). This suggests that movement along some of the major shear zones in the region, evident in the magnetic intensity image, could be responsible for the younger ages for the biotite in the vicinity of Cairn Hill.

Sample information and Locations:

Three samples only.

Sample number	Location	MGA East	MGA North	Zone	Target mineral	Lithology
1978579	Cairn Hill mine	511919	6758775	53	honblende	altered granite
1998157	Cairn Hill mine	515330	6759520	53	phlogopite	magnetite ore
2131370	Drill hole KDD005, 130.5-131.9m	491100	6750371	53	biotite	quartzofeldspathic gneiss

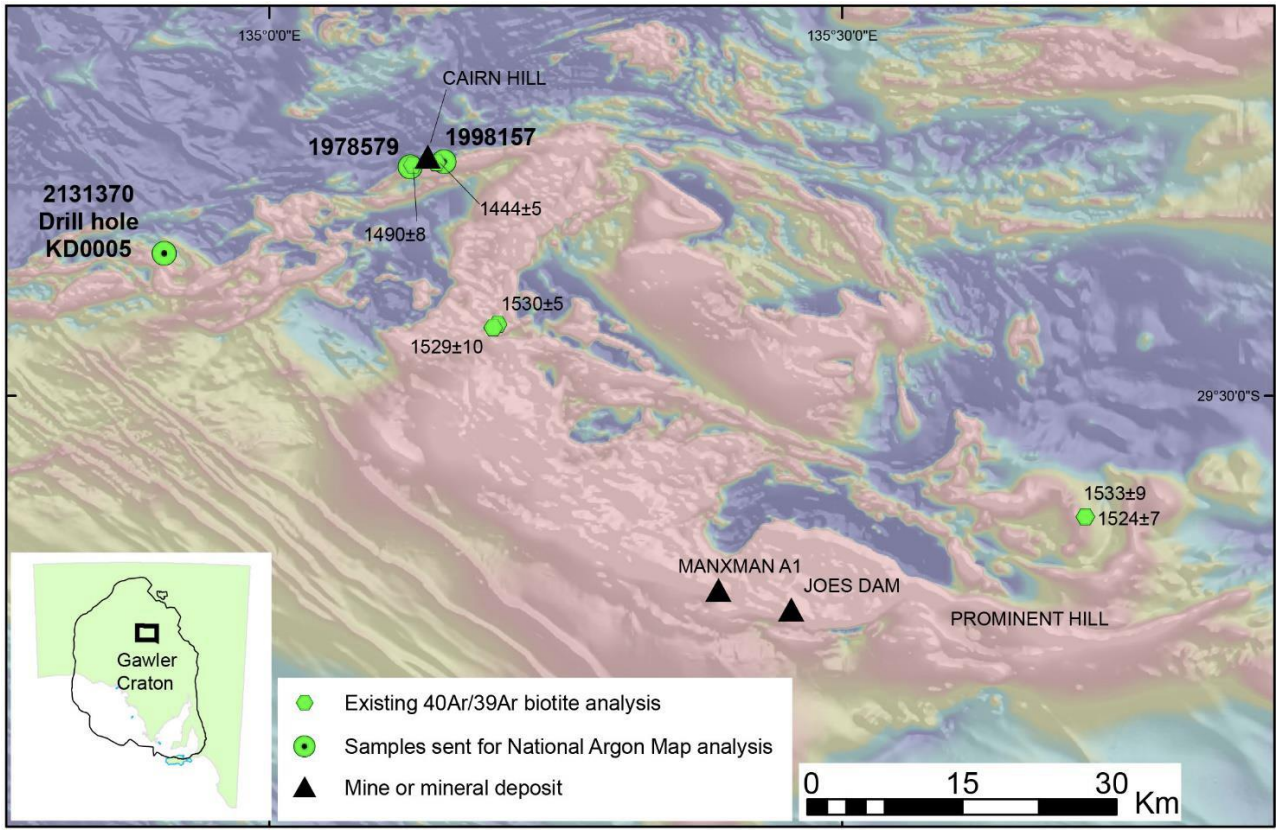

Location map of samples submitted for this National Argon Map application. Note the samples of biotite in the vicinity of Cairn Hill Mine are from Fraser et al. (2012); other samples are those of Forbes et al. (2012).

Sample Description and Rock Photograph

Sample 1978579 is a quartzofeldspathic gneiss with an emplacement age of 1572 ± 6 Ma with a vein of magnetite-amphibole (hornblende) alteration that cuts the main fabric. Thin section reveals the coarse-grained nature of the hornblende suitable for dating.

Sample 1998157 is a sample of coarse magnetite ore from Pit 1 of the Cairn Hill Mine. The sample contains very coarse magnetite crystals intergrown with phlogopite forming coarse mica books.

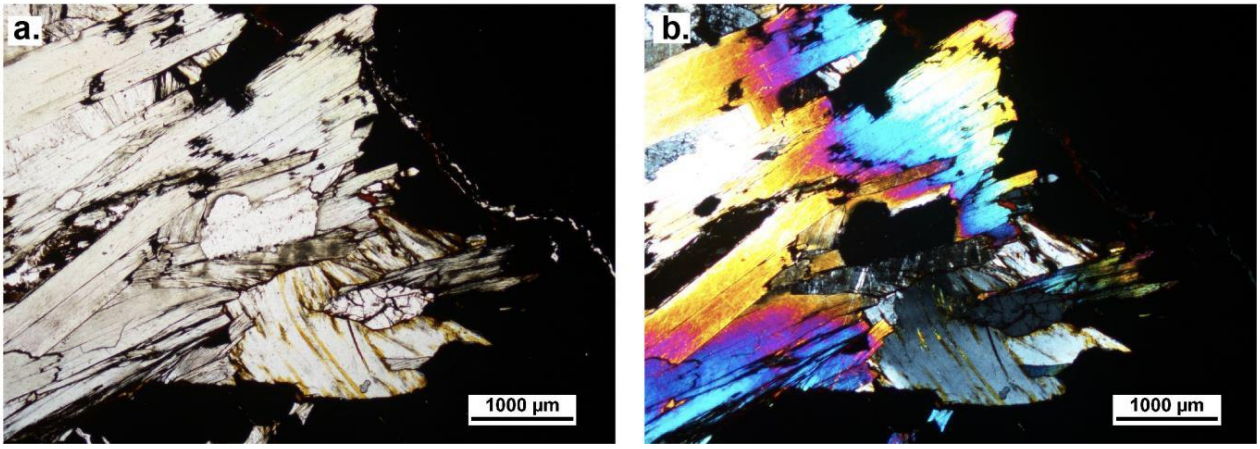

Photomicrographs of sample 1998157. a. Plain polarised light. b. Cross polars. Opaque mineral is massive magnetite.

Sample 2131370 is a biotite-bearing granitic gneiss. The sample is from the upper portion of drill hole KDD005, located to the west of Cairn Hill (Garsed et al., 2006). The drill hole intersected dark grey to black, and pink mafic and felsic gneisses in the upper part of the hole, with the lower unit (from about 250m) being dominated by pale grey quartz rich garnet gneiss. From around 230m to 252m is a dark grey to green, overprinting pyroxene-amphibole alteration. There is only minor sulphide mineralisation present in this hole.
Further samples could be taken from the amphibole alteration in this hole, or from others in the KDD series (Kangaroo Dam) pending results from the current round of analysis.

Photograph of sample 2131370.

$^{40}Ar/^{39}Ar$ analysis plots and information

The age plots are interpreted using the Asymptote and Limits method (Forster and Lister 2004). The argon system is affected by heat, for example if a sample is heated long enough then the argon system will be completely reset, if however, it is heated for a relatively short period of time and/or with temperatures that are not extreme then the sample may be only partially reset. Thus, relic ages can be retained and likewise overprinting events can be recorded and not overprint the argon system completely. As a consequence, the argon plots can have more than one 'age'. In many cases a minor overprinting event can be seen in these plots, it will be a maximum age and not necessary an accurate age but does show that a younger overprinting event did occur. It can be seen the youngest eventcan be followed by diffusional loss and/or mixing steps towards the older ages that are highlighted in green or blue for the older ages.

The argon data results are presented as Apparent Age Plots. The age data is presented on these plots showing the ages for different populations within each sample. Each age is highlighted and defined by a dashed orange line and shows the error, the MSWD, the steps representing the % gas release, and the Pearsons chi statistics for each of these domains is presented where applicable. There can be e.g. three ages defined on each spectrum: 1) the minor age defined (brown) at the low temperature of the experiment shows that there has been a minor overprinting event, but this age is not accurate and is only defined by e.g. <2% gas release. 2) intermediate domain/s (green), commonly this is the major gas release; 3) a relic domain age (blue) that has been preserved showing an older history occurred. The intervening steps that are yellow or clear represent mixing steps and are a normal phenomenon. In addition, listed are the sample identification number; the foil number; the mineral; the ANU canister number; the mass used and the number of steps. At the base of the plot is the sample information e.g. location.

Summary: Each of the selected interpreted ages have been labelled with a dashed orange line and the age and age data placed on that line. This includes the age, the calculated error, the MSWD and all to 95% c.l. These blue or green selected steps represent an age population. Note that in several cases the mixing steps are yellow (this is a software aspect and is meaningless).

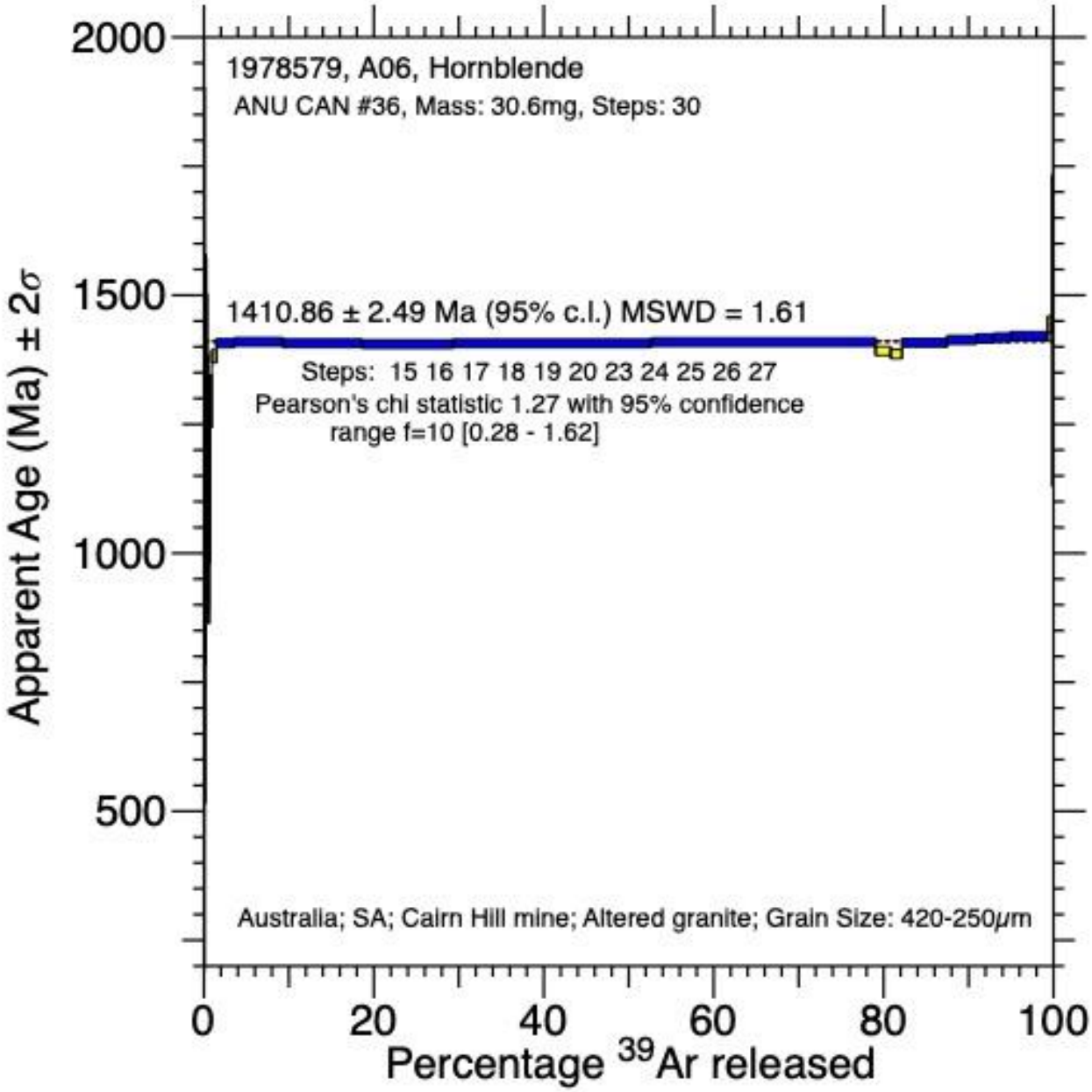
1978579, A06, Hornblende
ANU CAN #36, Mass: 30.6mg, Steps: 30
1410.86 ± 2.49 Ma (95% c.l.) MSWD = 1.61
Steps: 15 16 17 18 19 20 23 24 25 26 27
Pearson's chi statistic 1.27 with 95% confidence
range f=10 [0.28 - 1.62]
Australia; SA; Cairn Hill mine; Altered granite; Grain Size: 420-250μm
Apparent Age (Ma) ± 2σ
2000
1500
1000
500
0
20
40
60
80
100
Percentage 39Ar released

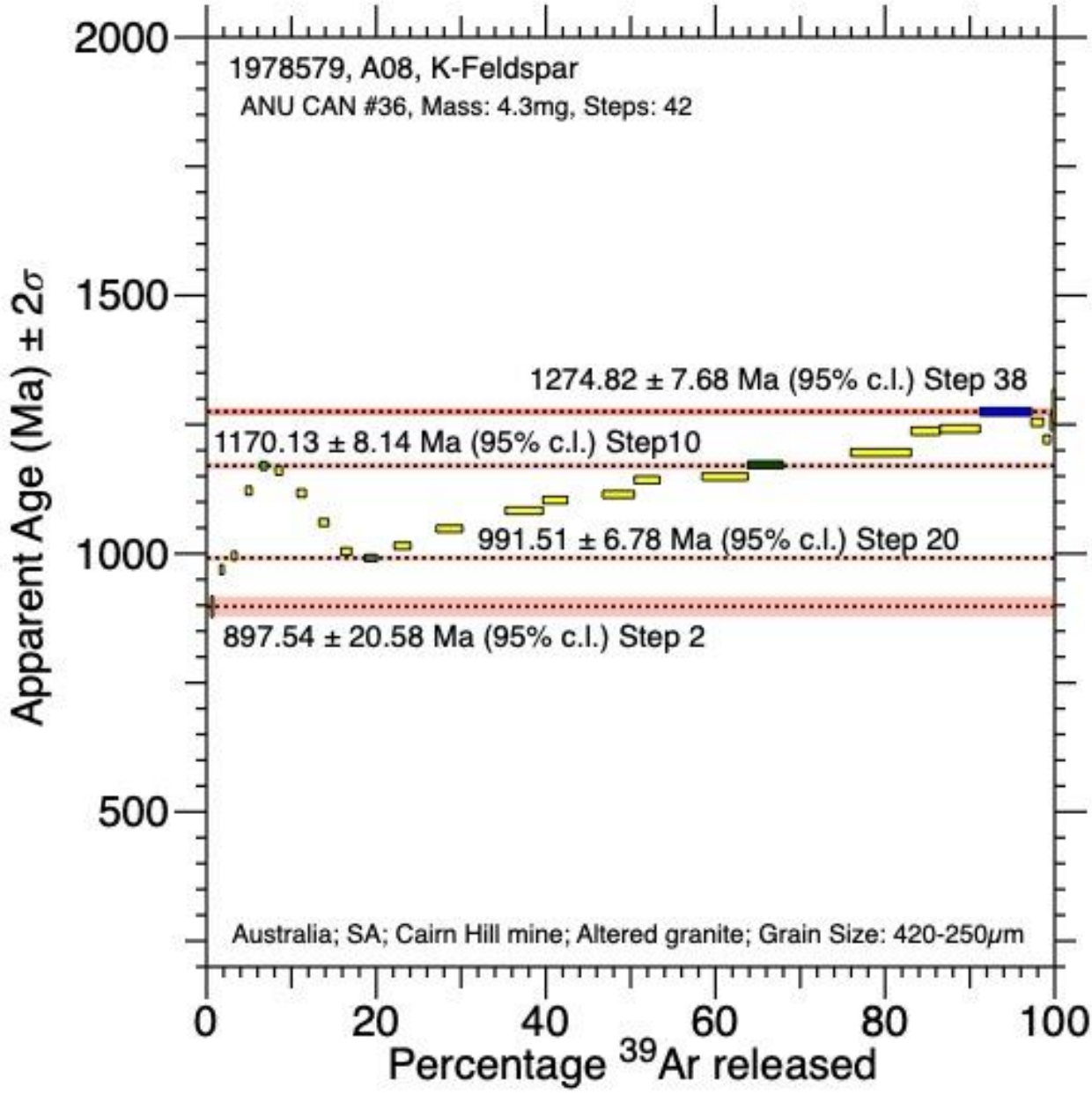
1978579, A08, K-Feldspar
ANU CAN #36, Mass: 4.3mg, Steps: 42
1274.82 ± 7.68 Ma (95% c.l.) Step 38
1170.13 ± 8.14 Ma (95% c.l.) Step10
991.51 ± 6.78 Ma (95% c.l.) Step 20
897.54 ± 20.58 Ma (95% c.l.) Step 2
Australia; SA; Cairn Hill mine; Altered granite; Grain Size: 420-250μm
Apparent Age (Ma) ± 2σ
Percentage 39Ar released
2000
1500
1000
500
0
20
40
60
80
100

UNSUCCESSFUL ANALYSIS

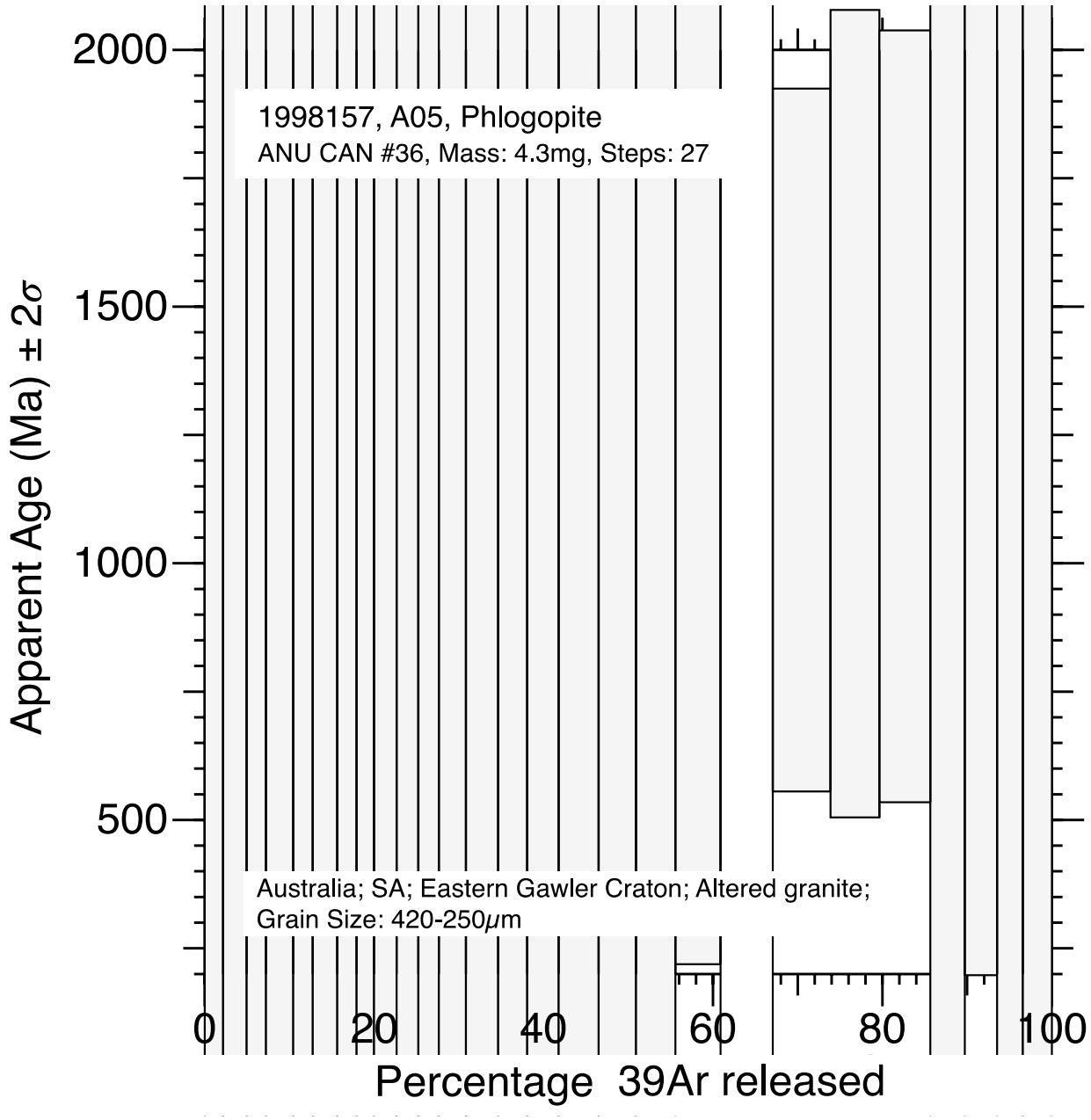

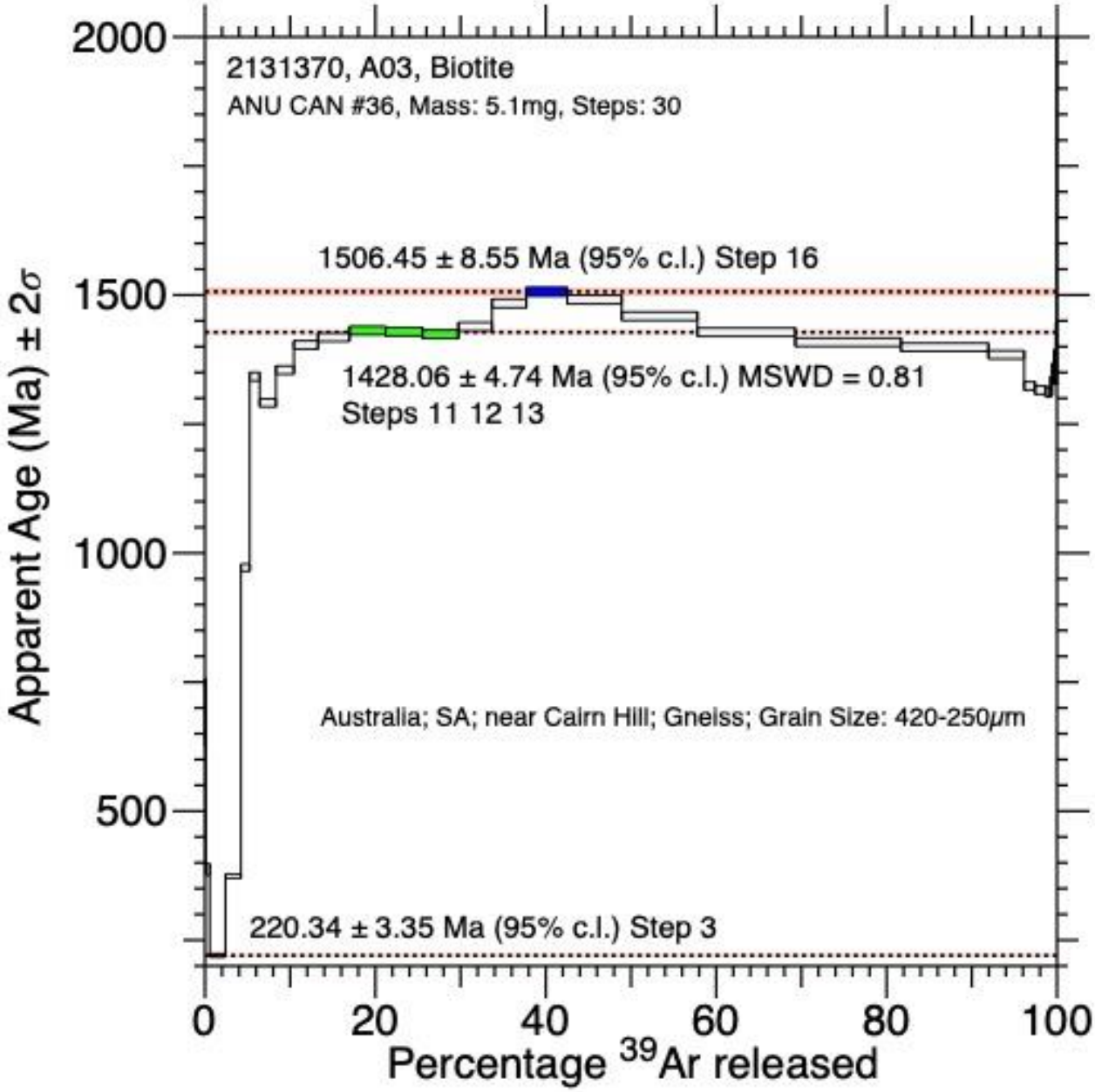
2131370, A03, Biotite
ANU CAN #36, Mass: 5.1mg, Steps: 30
1506.45 ± 8.55 Ma (95% c.l.) Step 16
1428.06 ± 4.74 Ma (95% c.l.) MSWD = 0.81
Steps 11 12 13
Australia; SA; near Cairn Hill; Gneiss; Grain Size: 420-250μm
220.34 ± 3.35 Ma (95% c.l.) Step 3
Apparent Age (Ma) ± 2σ
2000
1500
1000
500
0
20
40
60
80
100
Percentage 39Ar released

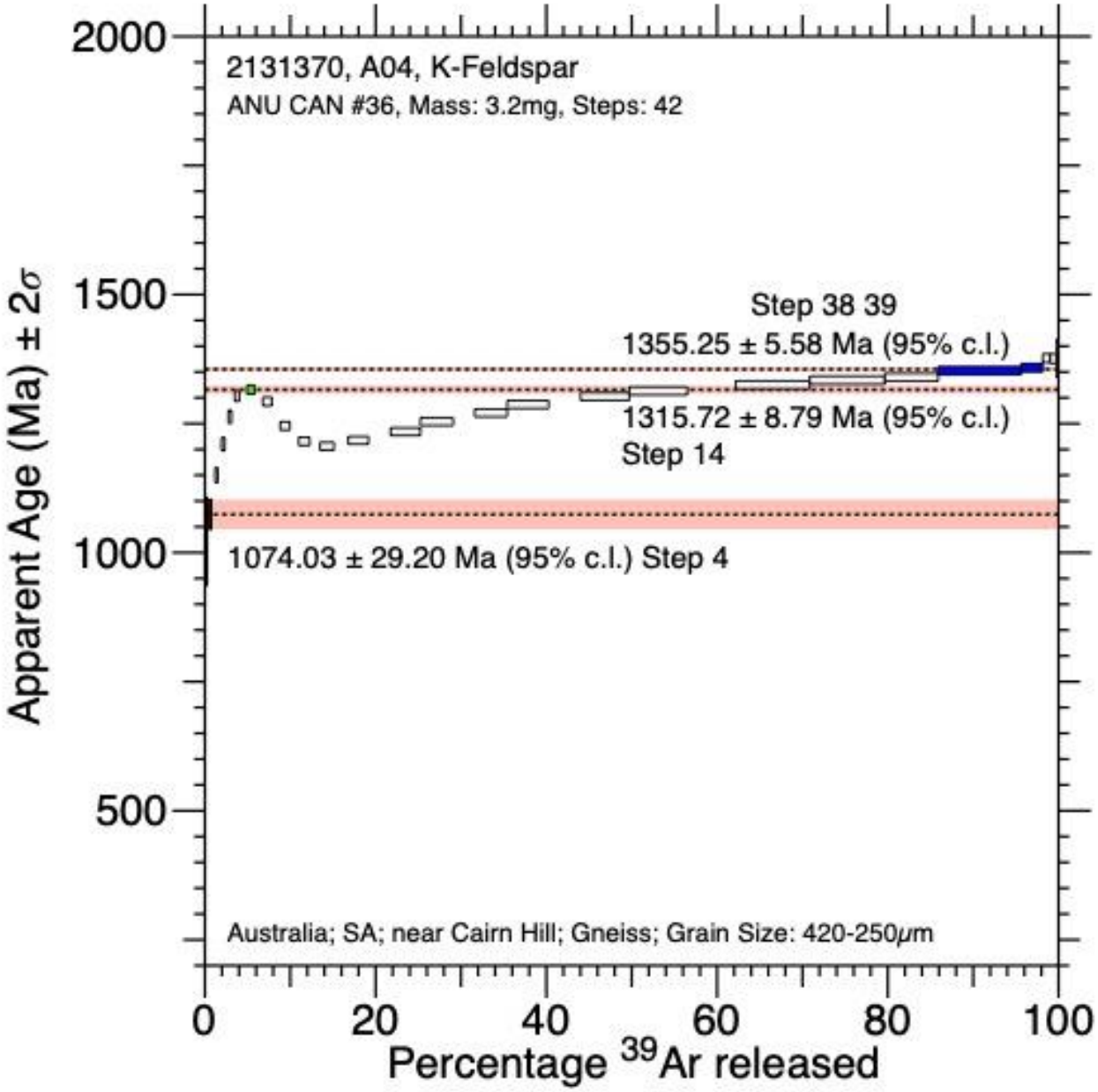
2131370, A04, K-Feldspar
ANU CAN #36, Mass: 3.2mg, Steps: 42
Step 38 39
1355.25 ± 5.58 Ma (95% c.l.)
1315.72 ± 8.79 Ma (95% c.l.)
Step 14
1074.03 ± 29.20 Ma (95% c.l.) Step 4
Australia; SA; near Cairn Hill; Gneiss; Grain Size: 420-250μm
Apparent Age (Ma) ± 2σ
2000
1500
1000
500
0
20
40
60
80
100
Percentage 39Ar released

Additional plots:

The following pages include nine different plots for each sample:

- Apparent Age Spectrum
- Arrhenius Plot (these are an estimate only).
- r/r0 Plot
- Percentage Radiogenic Argon
- Ca/K Plot
- Cl/K Plot
- Turner Plot

These are provided to enhance the understanding of the analytical results.

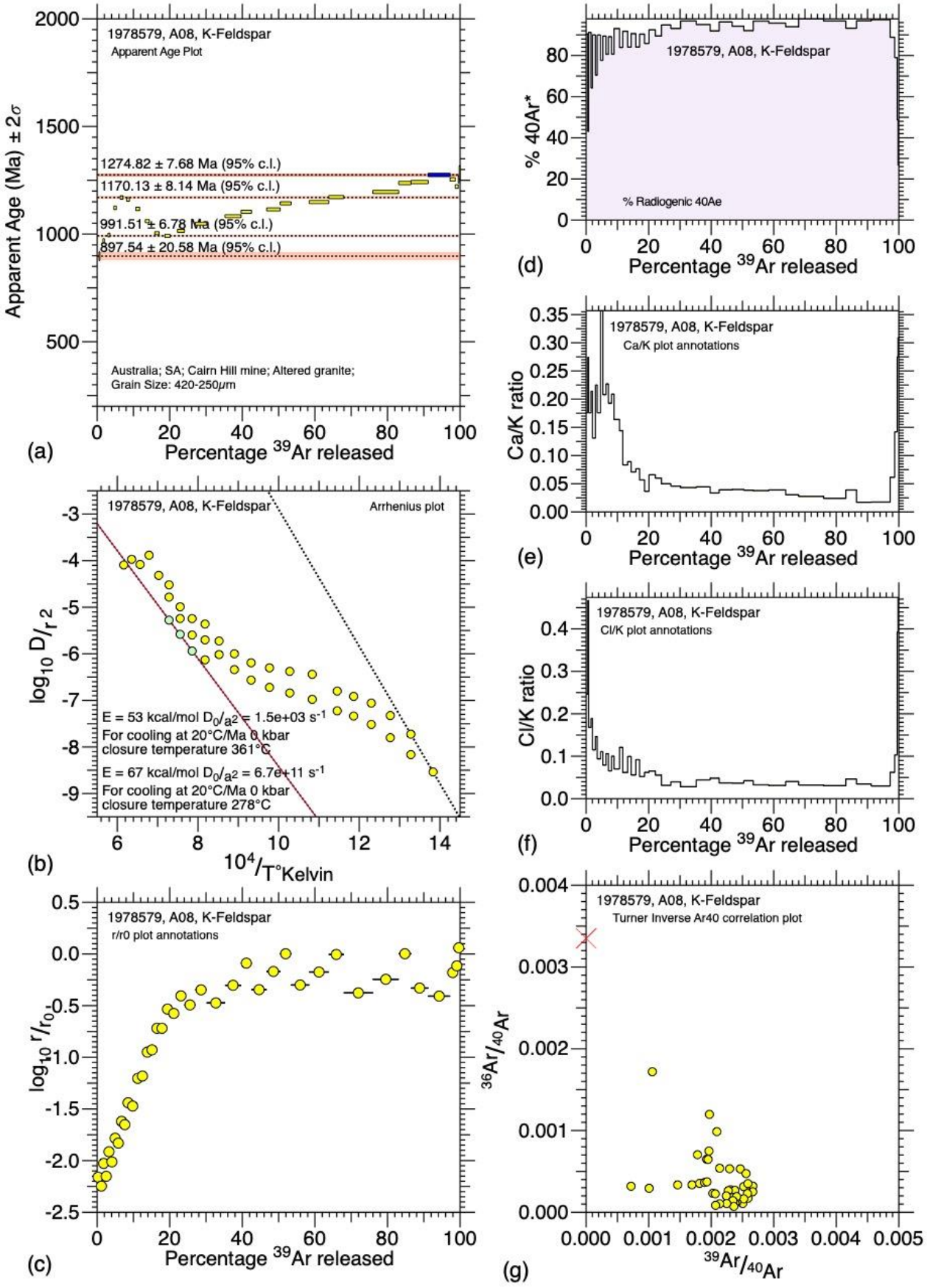
1978579, A08, K-Feldspar
Apparent Age Plot
1274.82 ± 7.68 Ma (95% c.l.)
1170.13 ± 8.14 Ma (95% c.l.)
991.51 ± 6.78 Ma (95% c.l.)
897.54 ± 20.58 Ma (95% c.l.)
Australia; SA; Cairn Hill mine; Altered granite;
Grain Size: 420-250μm
Apparent Age (Ma) ± 2σ
Percentage 39Ar released
(a)
1978579, A08, K-Feldspar
Arrhenius plot
E = 53 kcal/mol D0/a2 = 1.5e+03 s-1
For cooling at 20°C/Ma 0 kbar
closure temperature 361°C
E = 67 kcal/mol D0/a2 = 6.7e+11 s-1
For cooling at 20°C/Ma 0 kbar
closure temperature 278°C
log10 D/r2
10^4/T°Kelvin
(b)
1978579, A08, K-Feldspar
r/r0 plot annotations
log10 r/r0
Percentage 39Ar released
(c)
1978579, A08, K-Feldspar
% Radiogenic 40Ae
% 40Ar*
Percentage 39Ar released
(d)
1978579, A08, K-Feldspar
Ca/K plot annotations
Ca/K ratio
Percentage 39Ar released
(e)
1978579, A08, K-Feldspar
Cl/K plot annotations
Cl/K ratio
Percentage 39Ar released
(f)
1978579, A08, K-Feldspar
Turner Inverse Ar40 correlation plot
36Ar/40Ar
39Ar/40Ar
(g)

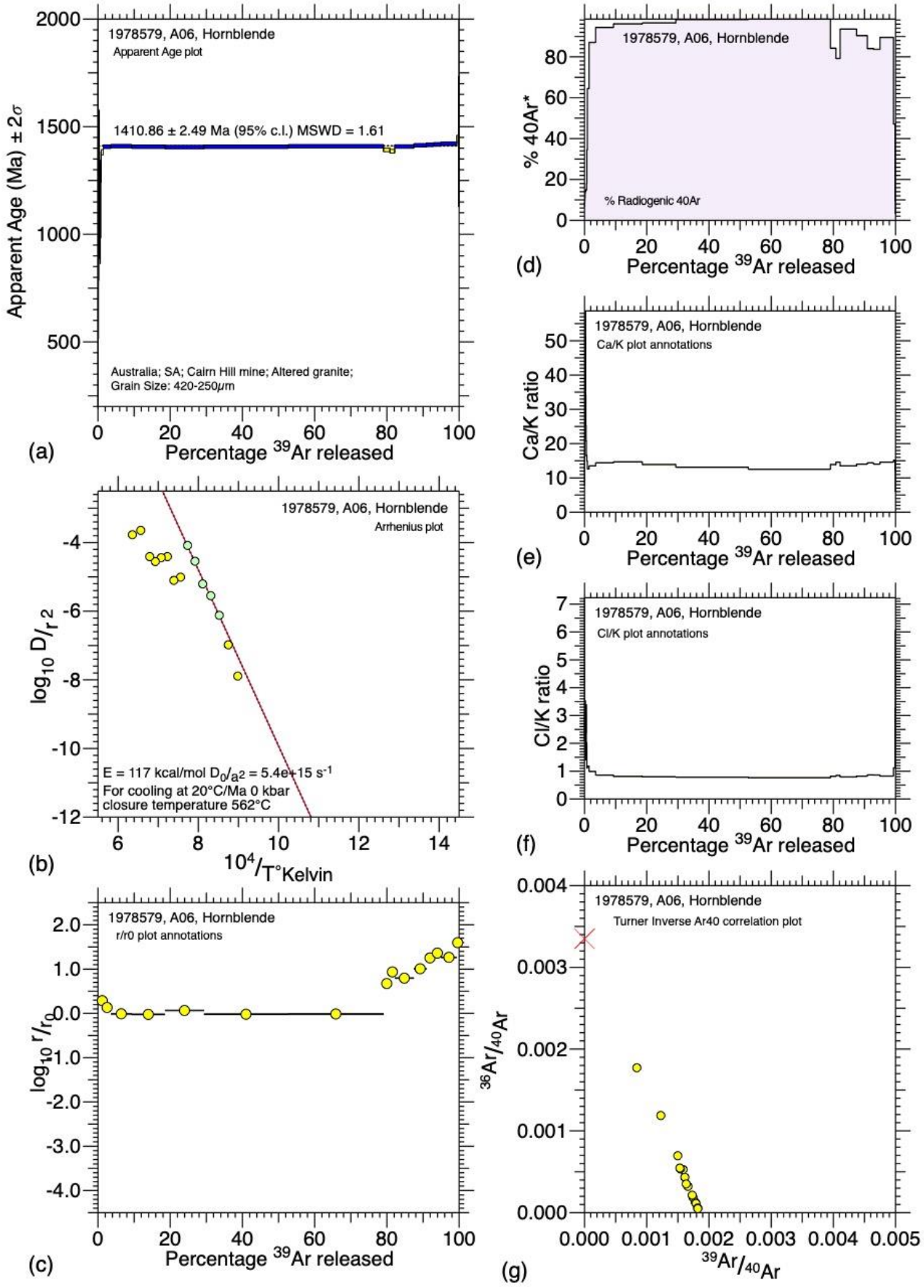
1978579, A06, Hornblende
Apparent Age plot
1410.86 ± 2.49 Ma (95% c.l.) MSWD = 1.61
Australia; SA; Cairn Hill mine; Altered granite;
Grain Size: 420-250μm
Apparent Age (Ma) ± 2σ
Percentage 39Ar released
(a)
1978579, A06, Hornblende
Arrhenius plot
E = 117 kcal/mol D0/a2 = 5.4e+15 s-1
For cooling at 20°C/Ma 0 kbar
closure temperature 562°C
log10 D/r2
10^4/T°Kelvin
(b)
1978579, A06, Hornblende
r/r0 plot annotations
log10 r/r0
Percentage 39Ar released
(c)
1978579, A06, Hornblende
% Radiogenic 40Ar
% 40Ar*
Percentage 39Ar released
(d)
1978579, A06, Hornblende
Ca/K plot annotations
Ca/K ratio
Percentage 39Ar released
(e)
1978579, A06, Hornblende
Cl/K plot annotations
Cl/K ratio
Percentage 39Ar released
(f)
1978579, A06, Hornblende
Turner Inverse Ar40 correlation plot
36Ar/40Ar
39Ar/40Ar
(g)

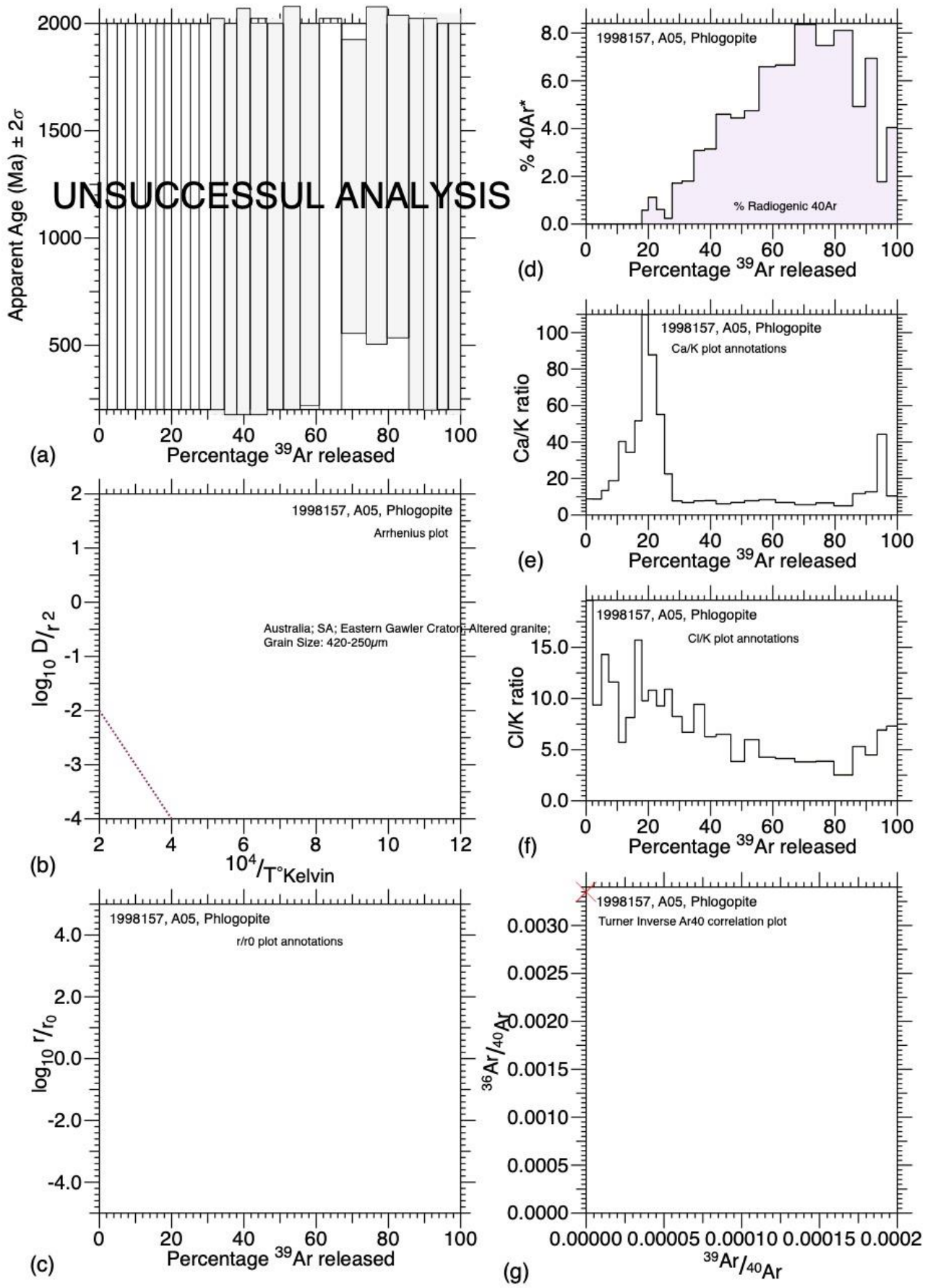
UNSUCCESSUL ANALYSIS
Apparent Age (Ma) ± 2σ
Percentage 39Ar released
(a)
1998157, A05, Phlogopite
Arrhenius plot
Australia; SA; Eastern Gawler Craton; Altered granite;
Grain Size: 420-250μm
log10 D/r2
10^4/T°Kelvin
(b)
1998157, A05, Phlogopite
r/r0 plot annotations
log10 r/r0
Percentage 39Ar released
(c)
1998157, A05, Phlogopite
% Radiogenic 40Ar
% 40Ar*
Percentage 39Ar released
(d)
1998157, A05, Phlogopite
Ca/K plot annotations
Ca/K ratio
Percentage 39Ar released
(e)
1998157, A05, Phlogopite
Cl/K plot annotations
Cl/K ratio
Percentage 39Ar released
(f)
1998157, A05, Phlogopite
Turner Inverse Ar40 correlation plot
36Ar/40Ar
39Ar/40Ar
(g)

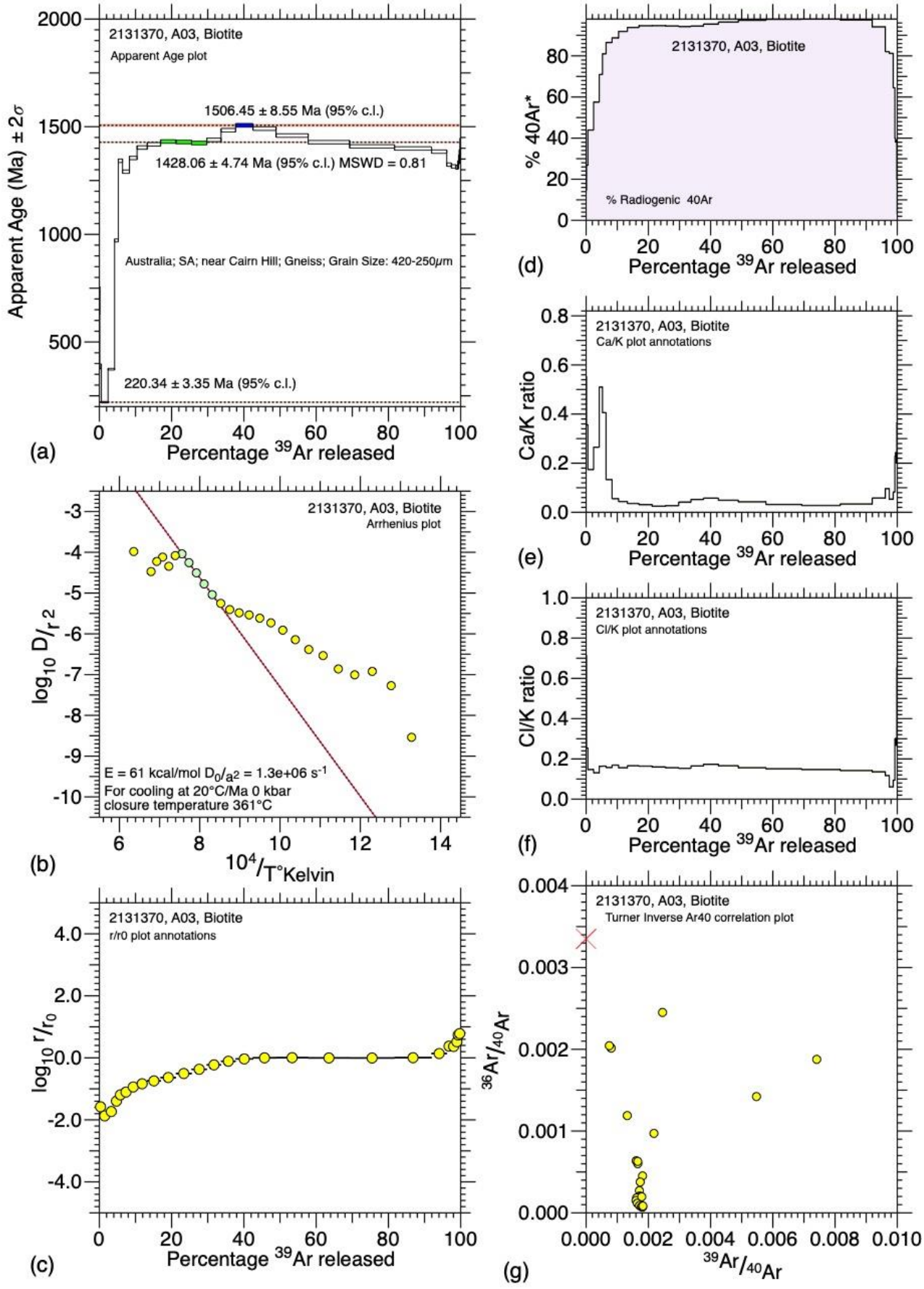
2131370, A03, Biotite
Apparent Age plot
1506.45 ± 8.55 Ma (95% c.l.)
1428.06 ± 4.74 Ma (95% c.l.) MSWD = 0.81
Australia; SA; near Cairn Hill; Gneiss; Grain Size: 420-250μm
220.34 ± 3.35 Ma (95% c.l.)
Apparent Age (Ma) ± 2σ
Percentage 39Ar released
(a)
2131370, A03, Biotite
Arrhenius plot
E = 61 kcal/mol D0/a2 = 1.3e+06 s-1
For cooling at 20°C/Ma 0 kbar
closure temperature 361°C
log10 D/r2
10^4/T°Kelvin
(b)
2131370, A03, Biotite
r/r0 plot annotations
log10 r/r0
Percentage 39Ar released
(c)
2131370, A03, Biotite
% Radiogenic 40Ar
% 40Ar*
Percentage 39Ar released
(d)
2131370, A03, Biotite
Ca/K plot annotations
Ca/K ratio
Percentage 39Ar released
(e)
2131370, A03, Biotite
Cl/K plot annotations
Cl/K ratio
Percentage 39Ar released
(f)
2131370, A03, Biotite
Turner Inverse Ar40 correlation plot
36Ar/40Ar
39Ar/40Ar
(g)

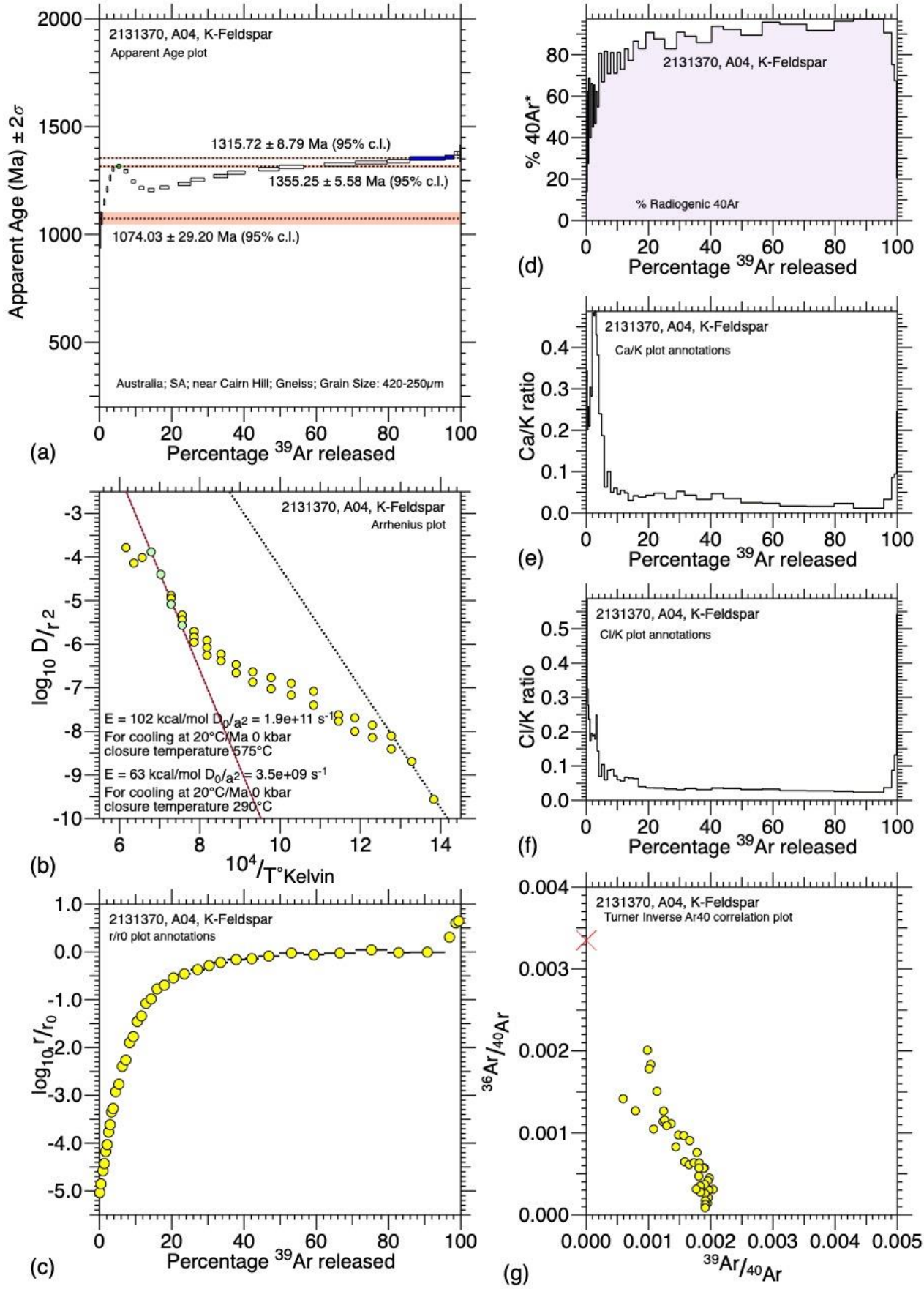
2131370, A04, K-Feldspar
Apparent Age plot
1315.72 ± 8.79 Ma (95% c.l.)
1355.25 ± 5.58 Ma (95% c.l.)
1074.03 ± 29.20 Ma (95% c.l.)
Australia; SA; near Cairn Hill; Gneiss; Grain Size: 420-250μm
Apparent Age (Ma) ± 2σ
Percentage 39Ar released
(a)
2131370, A04, K-Feldspar
Arrhenius plot
E = 102 kcal/mol D0/a2 = 1.9e+11 s-1
For cooling at 20°C/Ma 0 kbar
closure temperature 575°C
E = 63 kcal/mol D0/a2 = 3.5e+09 s-1
For cooling at 20°C/Ma 0 kbar
closure temperature 290°C
log10 D/r2
10^4/T°Kelvin
(b)
2131370, A04, K-Feldspar
r/r0 plot annotations
log10 r/r0
Percentage 39Ar released
(c)
2131370, A04, K-Feldspar
% Radiogenic 40Ar
% 40Ar*
Percentage 39Ar released
(d)
2131370, A04, K-Feldspar
Ca/K plot annotations
Ca/K ratio
Percentage 39Ar released
(e)
2131370, A04, K-Feldspar
Cl/K plot annotations
Cl/K ratio
Percentage 39Ar released
(f)
2131370, A04, K-Feldspar
Turner Inverse Ar40 correlation plot
36Ar/40Ar
39Ar/40Ar
(g)

Supplementary Data:

ANU Argon Facility Technical Report: ANU13-2020 & ANU14-2020
40Ar/39Ar Analysis for National Argon Map
By Marnie Forster and Davood Vasegh

NAM Proposals 02, 03 and 04:

- **Dating of mineralisation-related alteration in the Olympic Cu-Au Province, Gawler Craton**
- **Dating of mineralisation-related alteration at the Cairn Hill Mine, and regional thermal history of the northern Mt Woods Region, Gawler Craton**
- **Reconnaissance thermochronology of Curnamona Province**

Methods and procedures

Sample selection and mineral separation:

The samples in this study were provided by Geological Survey of South Australia and the separation procedures were undertaken in rock crushing and mineral separation laboratories at The Australian National University (Table 1). No chemical or leaching treatments were used during separation.
Mineral separation begins by choosing the most pristine sections with no evidence of weathering or staining. For samples with a targeted microstructure, the rock is first sliced into thin slabs using a trim saw, the selected area was then cut from the rock using a band saw. Once the selected area was separated, it was then crushed, milled and de-slimed as many times as was necessary to clean the grains and finally washed in deionised water.

K-feldspar procedure:

For these minerals the grains are sieved into size fractions: 250-420µm and passed through 0.25A then 1.0A current using a Frantz magnetic separator. K-feldspars are concentrated in the non-magnetic 1A fraction. This grain fraction is then separated under gravity using the Lithium heteropolytungstates (aq) (LST) heavy liquid at 2.58 g/cm3. K-feldspars are concentrated in the lighter than 2.58 g/cm3 size fraction. The separated grains are washed as many times as was necessary to remove any residue LST on the grains with deionised water. Final hand-picking of the best quality grains was done in the Argon Preparation Laboratory.

White Mica (Muscovite) procedure:

For these minerals the grains are sieved into size fractions: 250-420µm, based on actual grain size in the sample. Additional white mica is obtained through 0.25A then 1.0A current using a Frantz magnetic separator. Final hand-picking of the best quality grains was done in the Argon Preparation Laboratory.

Biotite (Phlogopite) procedure:

For these minerals the grains are sieved into size fractions: 250-420µm, based on actual grain size in the sample. Paper concentration is performed on the 250-420 µm size fraction to obtain the purest mineral separation as possible. Additional biotite is obtained by separating grains through 0.25A current using a Frantz magnetic separator, with biotite concentrated in the magnetic 0.25A fraction. Final hand-picking of the best quality grains was done in the Argon Preparation Laboratory.

Hornblende procedure:

For these minerals the grains are sieved into size fractions: 250-420µm based on actual grain size. Grains in the 250-420 µm size fraction is selected and passed through 0.25A current using a Frantz magnetic separator. Hornblendes are concentrated in the magnetic 0.25A fraction. If the separates from FRANTZ are not pure (i.e. ≥ 50% hornblende), this grain fraction is then separated

under gravity using the Lithium heteropolytungstates (aq) (LST) heavy liquid at 2.9 g/cm3. Hornblendes are concentrated in the heavier than 2.9 g/cm3 size fraction. The separated grains are washed as many times as was necessary to remove any residue LST on the grains with deionized water Final hand-picking of the best quality grains was done in the Argon Preparation Laboratory.

Mineral separation details:

Sample ID	Target Mineral	Mass (mg)	Grain Size (µm)	Treatment / Comment	Picture
2131356	Muscovite	3.2	420-250	Chloritised mica crystals with green-black hue	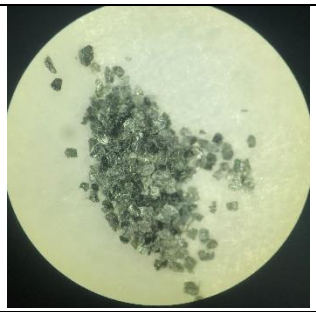
2111462	K-feldspar	4.4	420-250	Dark orange K-feldspar crystals, pure fraction	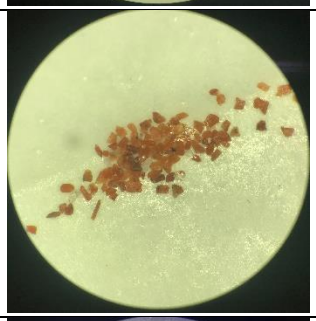
2131370	Biotite	4.9	420-250	Shiny black biotite crystals, pure fraction	
2131370	K-feldspar	3.3	420-250	White and orange K-feldspar crystals with rare tiny dark inclusions, clean fraction.	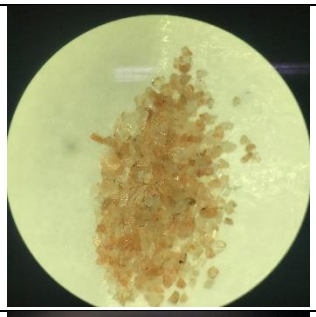
1998157	Phlogopite	4.3	420-250	Dark black phlogopite aggregates with dull sheen.	

1978579	Hornblende	30.8	420-250	Clean prismatic hornblende crystals, pure fraction	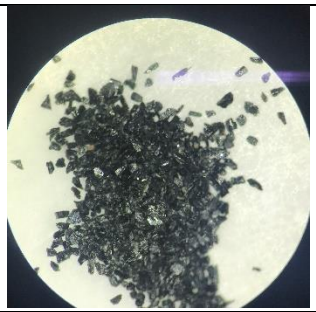
1978579	K-feldspar	3.8	420-250	Creamy white-orange K-feldspar crystals, pure fraction	
2016096	Muscovite	3.1	420-250	Shiny white-mica crystals with rare dark inclusions, clean fraction	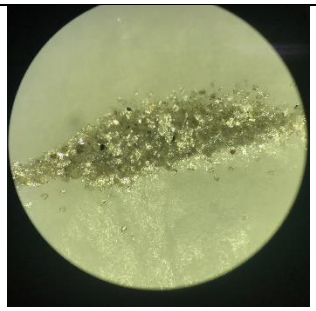
2016096	Biotite	4.2	420-250	Shiny black biotite crystals in a mixture with some white-mica and quartz crystals	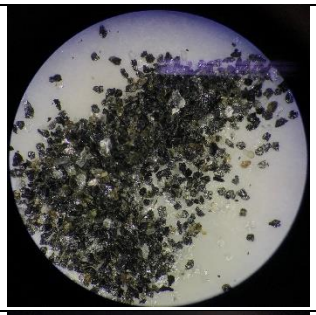
2016087	Muscovite	2.6	420-250	Shiny white-mica crystals, pure fraction	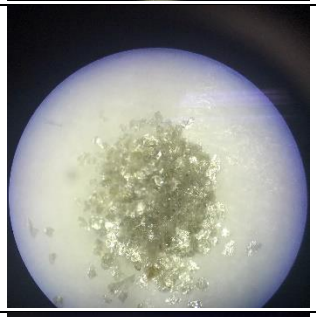
2016087	Biotite	4.8	420-250	Shiny black biotite crystals, pure fraction	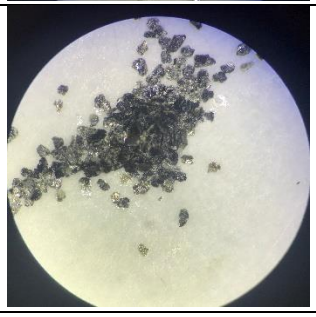

2016108	Muscovite	3.7	420-250	Shiny white-mica crystals, pure fraction	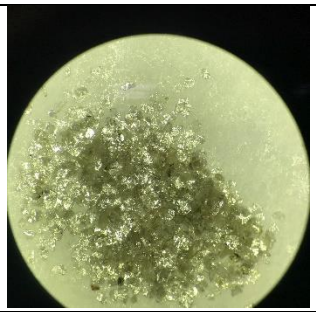
2016108	Biotite	4.4	420-250	Shiny black biotite crystals, pure fraction	
1707876	Muscovite	3.2	420-250	Shiny white-mica crystals, pure fraction	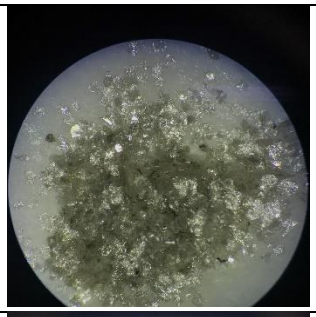
1707876	Biotite	4.7	420-250	Black-green chloritized biotite crystals, clean fraction	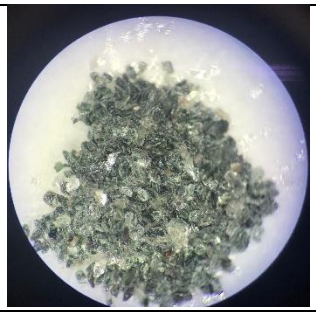

Table 1: Mineral separation details

Sample irradiation details:

Irradiation of samples for $^{40}Ar/^{39}Ar$ analysis was undertaken at the University of California Davis McClellan Nuclear Research Centre, CA, US in Central Facility position of TRIGA reactor without rotation, with 1.0mm of Cadmium shielding as ANU CAN #36 for 12.08 hours on 11-12 August 2020. The calculated amounts of grains were weighed and recorded and then wrapped in labelled aluminium packets in preparation for irradiation. The sample filled foils were placed into a quartz irradiation canister together with aliquots of the flux monitor Biotite GA1550. The foil packets of GA1550 standards were dispersed 6-8mm apart throughout the irradiation canister, between the unknown age samples. In addition, packets containing K_2SO_4 and CaF_2 were placed in the middle of the canister to monitor argon isotope production from potassium and other interfering elements.
Irradiated samples were unwrapped upon their return to the Australian National University, and then rewrapped in tin foils in preparation for analysis under vacuum in the furnace. Tin foil is used because the melting temperature of tin is lower than the experiment starting point in the furnace and gasses from tin can be pumped away prior to the sample analysis.

$^{40}Ar/^{39}Ar$ procedures and analysis information

Methodology:

Temperature-controlled resistance furnace step-heating experiments is the technique that is used in the ANU Argon laboratory to extract argon isotopes from the samples to ensure 100% release of ^{39}Ar. A sample is dropped into a cleaned furnace and heated to 400°C to melt the tin foil and then left in the furnace at 350°C for 8-12 hours to pump away unwanted gases. This cleaning procedure has proven to significantly improve the quality of the resultant data. The step-heating experiment then starts at 450°C, and each incremental heating step is heated at a constant temperature for 15 minutes. The heating process involves rapid heating to the setpoint temperature with no overshoot, then temperature is maintained for 15 minutes followed by rapid cooling; this procedure produces a square wave in temperature for each heating step. The heating step schedule for biotite and muscovite rises by 30°C increments (except for the last a few steps), with 30 steps per sample, while K-feldspar is analysed in more than 40 steps, including numerous isothermal steps. Diffusion experiments, as conducted in the ANU Argon laboratory, are designed to retrieve diffusion parameters which can be used in quantitative temperature-time modelling. The heating schedules are recorded in the Excel Tables for each sample.

Cleaning of the furnace between samples is vital in this method. The furnace is degassed four times at 1,450°C for 15 minutes and the gas pumped away prior to the loading of the subsequent sample. Blanks are measured to monitor the cleaning process. The flux monitor crystals are fused using a CO_2 continuous-wave laser. Gas released from either the flux monitors or each step of the sample analyses are exposed to three Zr-Al getters; two AP10 (Cold and hot) and one CP50, each for 10 minutes, to remove active gases. The purified extracted gasses are then isotopically analysed in the Argus VI mass spectrometer. The $^{40}Ar/^{39}Ar$ dating technique is adapted from McDougall and Harrison (1999) and described in Forster and Lister (2009).

Background levels are measured and subtracted from all analyses, from flux monitors and samples. The nuclear interfering values for the correction factors for the isotopes are listed below (Tetley et al 1980). These are measured for the reactions and uncertainties of $(^{36}Ar/^{37}Ar)_{Ca}$, $(^{39}Ar/^{37}Ar)_{Ca}$, $(^{40}Ar/^{39}Ar)_{K}$, $(^{38}Ar/^{39}Ar)_{K}$ and $(^{38}Ar)_{Cl}/(^{39}Ar)_{K}$, and were calculated prior to sample analyses.

Mass spectrometer setup and procedures

Samples and standards were analysed in the Argon Laboratory at the Research School of Earth Science, The Australian National University, Canberra, Australia using a *Thermo Fisher ARGUS-VI* multi-collector mass spectrometer (Table 2).

Mass Spectrometer:	Thermo Fisher Argus VI
Detector Type:	Faraday Cups only x5
Calibrations:	3 levels (Zero Offset, Gain and Cross Calibration)
Peak Centring:	Once for every measurement @H2 (^{40}Ar)
Measurement Cycles:	51 cycles on all detectors
Extrapolation Method:	Exponential extrapolation and uncertainty

Name	UFC Offset [fA]	Gain	Cross Calibration Factor
H2	-4.9761469	0.9871203	1
H1	-2.2071069	0.9671459	1.007184188
AX	-7.6814703	0.9769602	1.017518151
L1	-2.3979322	0.9706487	1.030604297
L2	-3.1329948	0.9676338	1.047244337

Table 2: Detector Calibration Values

The calculation parameters:

Lambda ^{40}K (Renne et al 2011)	5.5305E-10
Lambda ^{37}Ar (Kondev et al 2017)	1.9798E-02
Lambda ^{39}Ar (Kondev et al 2017)	7.0548E-06
Lambda ^{36}Cl (Kondev et al 2017)	6.2985E-09
Flux Monitor	GA1550 @ 99.18 ± 0.14 Ma
Total irradiation power	12.08 MW
Irradiation Date	11-12 Aug, 2020
Irradiation shielding	Cadmium 1.0mm

Interfering isotope production ratios:

$(^{36}Ar/^{37}Ar)_{Ca}$ correction factor	1.01283E-04
$(^{39}Ar/^{37}Ar)_{Ca}$ correction factor	8.46943E-03
$(^{40}Ar/^{39}Ar)_{K}$ correction factor	1.34009E-01
$(^{38}Ar/^{39}Ar)_{K}$ correction factor	1.05445E-02
$(^{38}Ar)_{Cl}/(^{39}Ar)_{K}$ correction factor	8.18472E-02
Ca/K conversion factor	1.90

Atmospheric Argon correction ratio:

$^{40}Ar/^{36}Ar$	(Lee et al 2006)	298.57
$^{40}Ar/^{38}Ar$	(Lee et al 2006)	1,583.52

Representative air shot and blanks measurements:

The discrimination factor was calculated by analysing five air shots on either side of sample analyses and is reported at 1amu. Table 3 shows an example of the analysed air shots and resultant calculation of discrimination factor.

Date	^{40}Ar ± %err		^{38}Ar ± %err		^{36}Ar ± %err		1amu ± %err		Reported Value
01-Dec-2020	1,851.556	0.015	1.379	2.326	6.313	0.567	1.00448	0.288	1.0048686 ± 0.213%
01-Dec-2020	1,848.823	0.015	1.310	2.894	6.354	0.633	1.00648	0.321	
01-Dec-2020	1,848.496	0.014	1.291	2.982	6.278	0.663	1.00349	0.336	
01-Dec-2020	1,845.605	0.013	1.372	2.566	6.276	0.691	1.00381	0.349	
01-Dec-2020	1,865.401	0.011	1.280	2.424	6.401	0.637	1.00608	0.323	

Table 3: Air Shots and Mass Discrimination Factor

The blank measurements are undertaken with different temperature schedules between 300°C and 1450°C, depending on the degassing behaviour and previous blank measurement results. The degassing and blank measurement procedure continues until the ratios of ^{40}Ar, ^{38}Ar and ^{36}Ar drop to atmospheric ratios, and ^{39}Ar and ^{37}Ar drop below detectable levels. The entire procedure of degassing and blank measurements is repeated at the end of a set of samples. Blanks will be done in-between samples that belong to a set, with reduced steps at 300°C, 1300°C and 1450°C to check isotope levels. In addition, the mass of each sample is calculated so that the volume of gas released from each step overwhelms the volume of gas that may occur in the blank. The table 4 is a representative sequence of measured blank values recorded during a monitoring process.

Temperature	^{40}Ar	^{39}Ar	^{38}Ar	^{37}Ar	^{36}Ar	$^{40}Ar/^{36}Ar$
300	1817.738	0.708661	1.209615	ND*	6.113996	297.3077
500	1879.391	0.741332	1.266375	ND	6.364901	295.2743

700	1911.306	0.759696	1.282523	0.095807	6.417252	297.8386
900	2053.27	0.775687	1.358664	ND	6.94095	295.8198
1100	2731.788	0.812587	1.788944	0.10454	9.192207	297.1852
1300	7305.089	1.038774	4.728446	0.139915	24.59727	296.9878
1450	36811.09	2.436249	23.78145	0.23653	124.4077	295.8909
300	748.5261	0.344558	0.467985	0.019884	2.5069	298.5864
1300	1126.281	0.438838	0.704102	0.0207706	3.744338	300.7958
1450	2181.428	1.00614	1.377076	0.1028531	7.299197	298.8587

Table 4: Example of the blanks measurements during a sequence of blanks where isotopes were being monitored prior to sample analysis (* => Not Detectable). Temperature is °C.

Data reduction software:

The calculations were done with an adapted version of *Noble* Software (2020, developed and adapted by the Australian National University Argon Laboratory) and all interpretations have been undertaken with *eArgon* (developed and adapted for ANU Argon Laboratory by G.S. Lister).

Reported Data:

The reported data have been corrected for system backgrounds, mass discrimination, fluence gradients and atmospheric contamination. GA1550 standards were analysed, and an exponential best fit was then used for the calculation of the J-factor and J-factor uncertainty (Table 5).

Samples J-Factor, Mass Discrimination, and uncertainties:

Sample Name	J-Factor ± %uncertainty		Mass Discrimination Factor ± %uncertainty		Measurement Date
2131356	2.18769E-03	0.2436	1.00485	0.142	13-Nov-2020
2111462	2.18596E-03	0.2436	1.00496	0.211	17-Nov-2020
2131370	2.18422E-03	0.2436	1.00496	0.211	22-Nov-2020
2131370	2.18248E-03	0.2436	1.00496	0.211	24-Nov-2020
1998157	2.18074E-03	0.2436	1.00487	0.213	27-Nov-2020
1978579	2.17901E-03	0.2436	1.00487	0.213	03-Dec-2020
1978579	2.17553E-03	0.2437	1.00499	0.142	05-Dec-2020
2016096	2.17380E-03	0.2437	1.00445	0.226	07-Dec-2020
2016096	2.17206E-03	0.2437	1.00445	0.226	10-Dec-2020
2016087	2.17032E-03	0.2437	1.00445	0.226	12-Dec-2020
2016087	2.16859E-03	0.2437	1.00430	0.197	15-Dec-2020
2016108	2.16685E-03	0.2437	1.00430	0.197	17-Dec-2020
2016108	2.16511E-03	0.2437	1.00403	0.103	19-Dec-2020
1707876	2.16338E-03	0.2437	1.00436	0.087	29-Dec-2020
1707876	2.16164E-03	0.2438	1.00436	0.087	30-Dec-2020

Table 5: Sample analysis and calculation details

$^{40}Ar/^{39}Ar$ isotopic data of the samples are supplied in the Excel Data Tables, which include details on the heating schedule, Argon isotopes abundances and their uncertainty levels, %Ar*, $^{40}Ar^*/^{39}Ar(K)$, Cumulative ^{39}Ar%, calculated age and its uncertainty, Ca/K, Cl/K, J-Factor and its uncertainty. Noting that all the reported uncertainties are at one sigma level and the fractional uncertainties are shown as % in the headings of the appropriate columns of data tables. The components involved in the calculation of the uncertainties are listed in Table 6.

Uncertainty of:	Components involved in the calculation
Isotope Abundances	Uncertainty of isotope measurement Uncertainty of Mass Discrimination Factor (except for ^{39}Ar)
J-Factor	Uncertainty of ^{40}K Decay Constant Uncertainty of Age of the Flux monitor Uncertainty of Flux monitor isotopes abundances
Calculated Age	Uncertainty of Isotopes Abundances J-Factor value and uncertainty of J-Factor ^{40}K Decay Constant value and uncertainty of ^{40}K Decay Constant

Table 6: Components involved in the calculation of each uncertainty

References:

Forster, M.A. and Lister, G.S. 2004. The interpretation of 40Ar/39Ar apparent age spectra produced by mixing: application of the method of asymptotes and limits. J*ournal of Structural Geology* **26,** 287–305

Forster, M.A. and Lister, G.S. 2009. Core-complex-related extension of the Aegean lithosphere initiated at the Eocene-Oligocene transition. *Journal Geophysical Research*, **114**, B02401.

McDougall, I. and Harrison, T.M. (Eds.). 1999. Geochronology and Thermochronology by the $^{40}Ar/^{39}Ar$ Method, 2nd ed., 269 pp. Oxford Univ. Press, New York.

Kondev, F.G. and Naimi, S. 2017. The NUBASE2016 evaluation of nuclear properties. *Chinese physics C*, **41**(3), p.030001.

Lee, J.Y., Marti, K., Severinghaus, J.P., Kawamura, K., Yoo, H.S., Lee, J.B. and Kim, J.S. 2006. A redetermination of the isotopic abundances of atmospheric Ar. *Geochimica et Cosmochimica Acta*, ***70***(17), 4507-4512.

Renne, P.R., Mundil, R., Balco, G., Min, K., and Ludwig, K.R. 2010. Joint determination of 40K decay constants and 40Ar*/40K for the Fish Canyon sanidine standard, and improved accuracy for 40Ar/39Ar geochronology. *Geochemica et Cosmochimica Acta,* **18**, 5349–5367.

Tetley, N., McDougall, I. & Heydegger, H.R. 1980. Thermal neutron interferences in the $^{40}Ar/^{39}Ar$ dating technique. *Journal Geophysical Research*, **85**, 7201–7205.